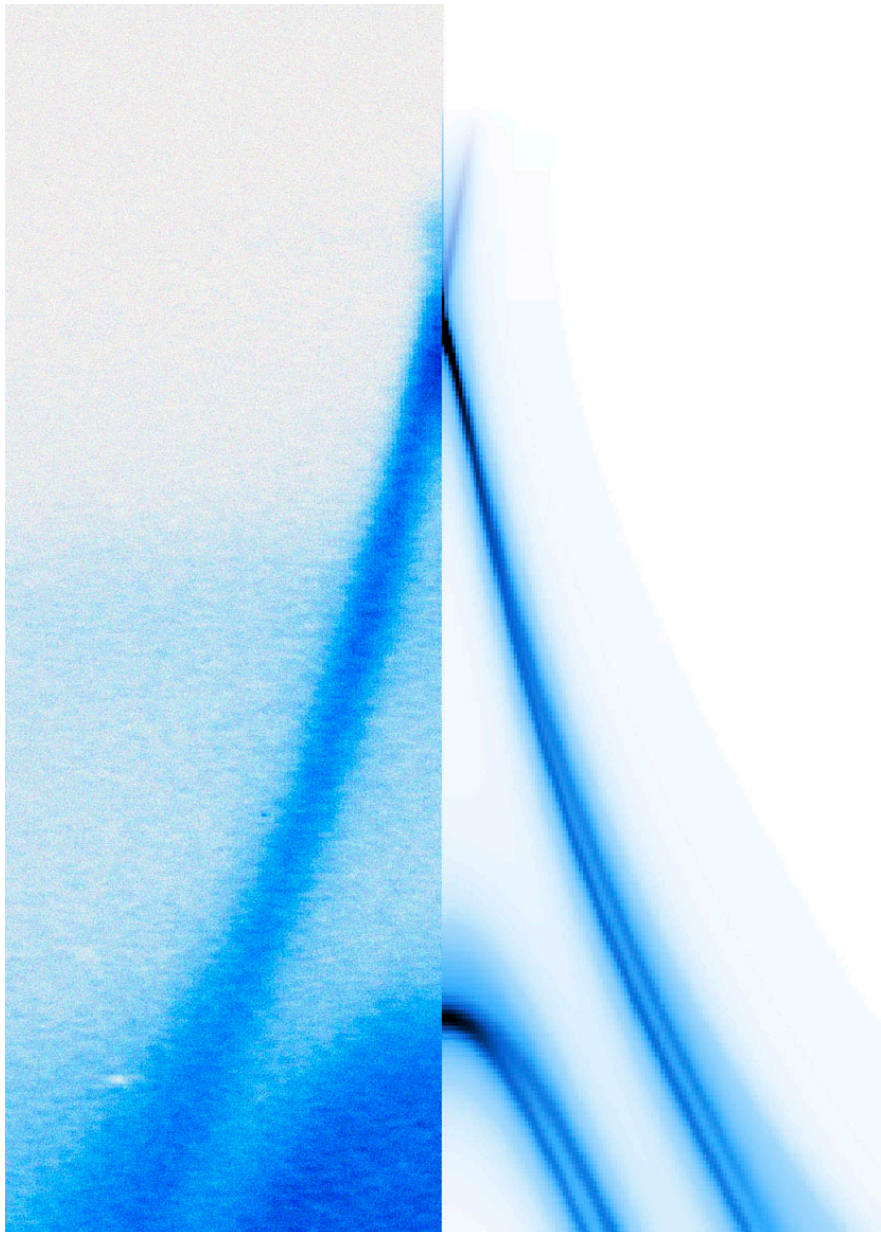

Spin-orbit interaction, topology and electronic structure

Oleg Yazyev

Chair of Computational Condensed Matter Physics (C3MP)

Institute of Physics (IPHYS)

Ecole Polytechnique Fédérale de Lausanne (EPFL)

Switzerland

Oleg Yazyev

Timeline of the field of topological materials

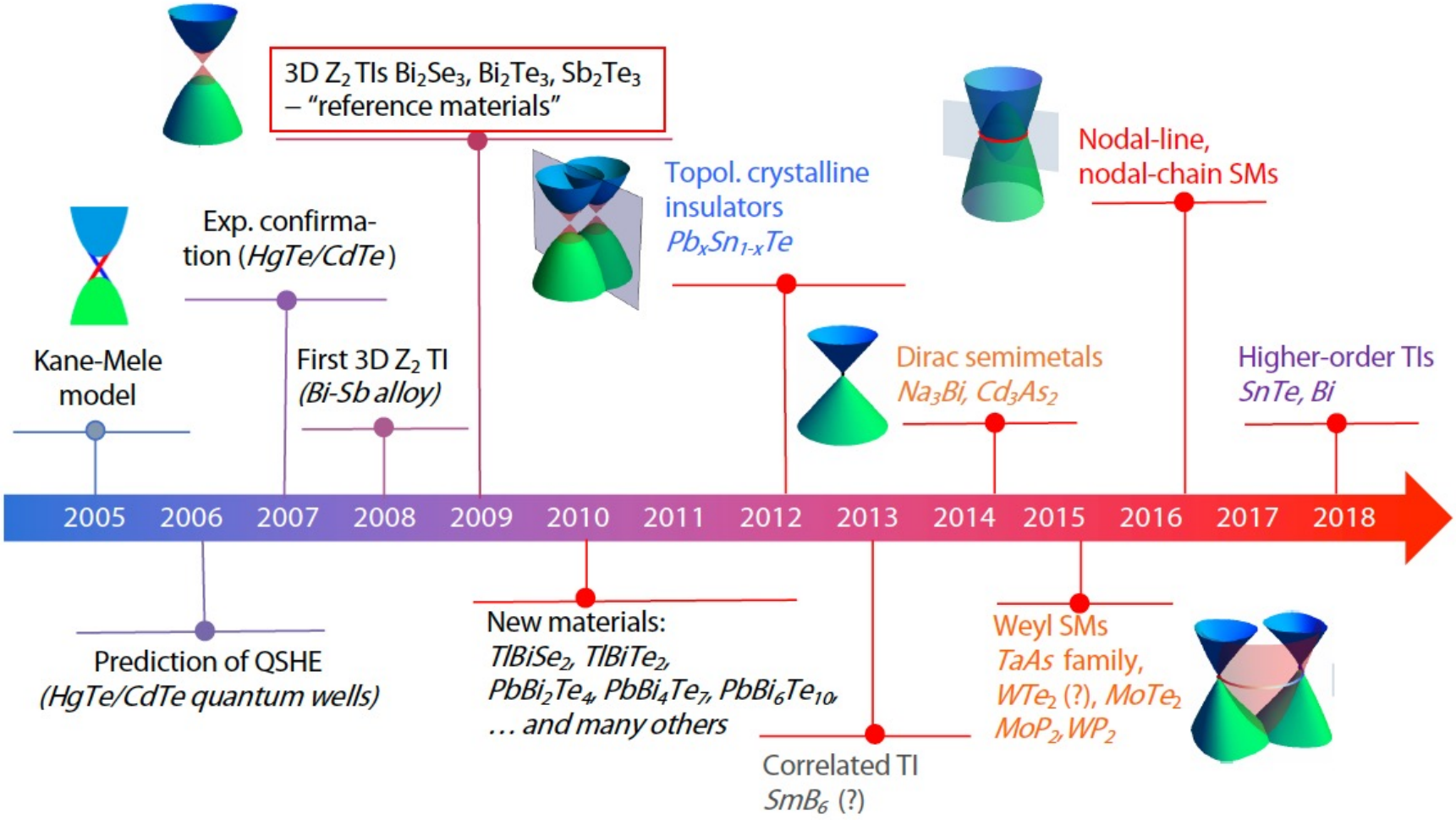

Talk outline

- Topological materials: brief introduction
- High-throughput search of novel topological materials

  online database TopoMat http://www.materialscloud.org/discover/topomat
- Discovery of new materials – successful examples:
  - Bi_4I_4 topological insulator

    G. Autès *et al.*, Nature Materials **15**, 154 (2016)
  - MoP_2 and WP_2 Weyl semimetals

    G. Autès *et al.*, Phys. Rev. Lett. **117**, 066402 (2016)
- "Textbook" physical properties – magnetoresistance

  S.N. Zhang, Q.S. Wu, Y. Liu, O. V. Yazyev, Phys. Rev. B **99**, 035142 (2019)
- Topological degeneracies and Fermi arcs in ordinary bcc iron

  D. Gosalbez-Martinez, G. Autés, O. V. Yazyev, Phys. Rev. B **102**, 035419 (2020)

Oleg Yazyev

Quantum Hall effect and Chern number

Bloch wavefunction: $\Psi_k(r) = e^{ikr} u_k(r)$

Berry connection: $A(k) = i\langle u_k | \nabla_k | u_k \rangle$

Berry phase: $\phi = \int_{\mathcal{P}} A(k) \mathrm{d}k$

Berry curvature: $B(k) = \nabla_k \times A(k)$

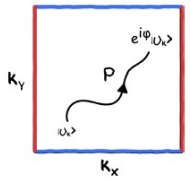

Theorem

The integral of $B(k)/2\pi$ over a closed surface is an integer $\mathcal{C}$.

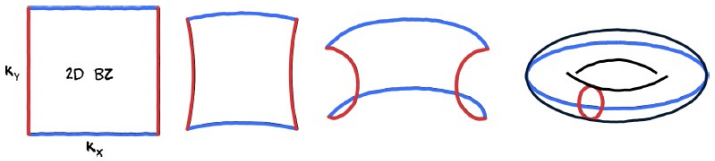

Chern number:

$$\mathcal{C} = \frac{1}{2\pi} \int_{\mathrm{2D\,BZ}} B(k) \mathrm{d}k \in \mathbb{Z}$$

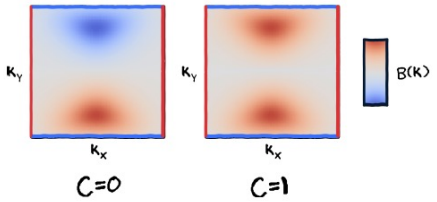

Integer quantum Hall effect (1980)

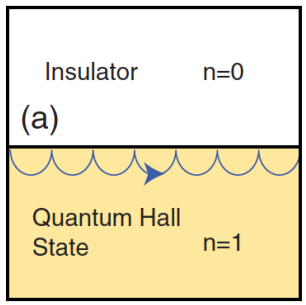

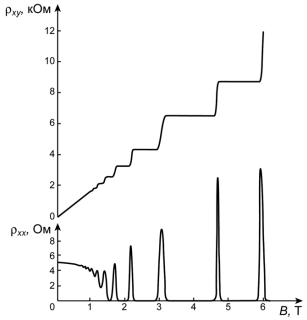

Haldane model

$$H = \sum_i M\tau_z c_i c_i^\dagger + \sum_{<i,j>} t_1 c_i c_j^\dagger + \sum_{<<i,j>>} t_2 e^{i\tau_z\phi} c_i c_j^\dagger$$

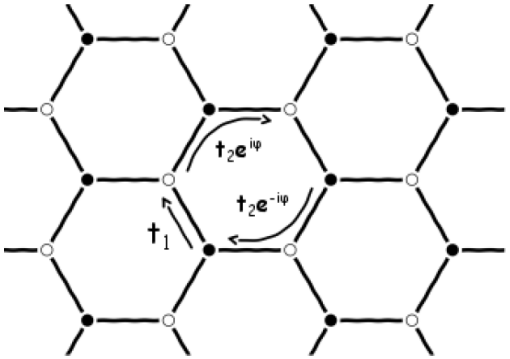

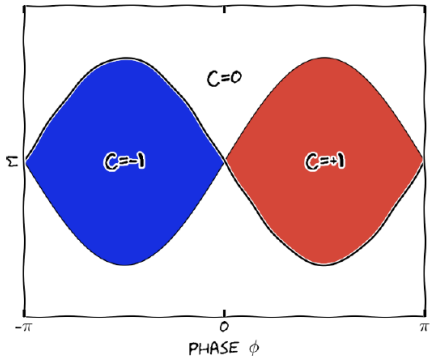

Haldane, Phys. Rev. Lett. **61**, 2015 (1988)

- breaks time-reversal symmetry
- chiral edge states
- integer quantum Hall effect without magnetic field (Chern insulator)

Quantum spin Hall effect

- Kane-Mele model – quantum spin Hall effect

$$H = \sum_{<i,j>} t c_{i\sigma} c^{\dagger}_{j\sigma} + \sum_{<<i,j>>} i\lambda \nu_{ij} c_i \sigma_z c^{\dagger}_j$$

- Z_2 topological invariant $\nu = \frac{\mathcal{C}_\uparrow - \mathcal{C}_\downarrow}{2} \in \{0, 1\}$

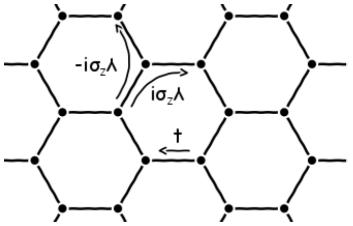

Kane & Mele, PRL 95, 226801 (2005)

- Corresponds to graphene + spin-orbit coupling (SOC)

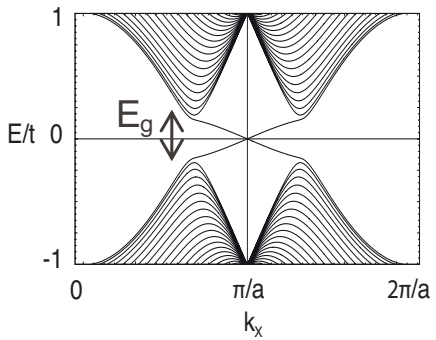

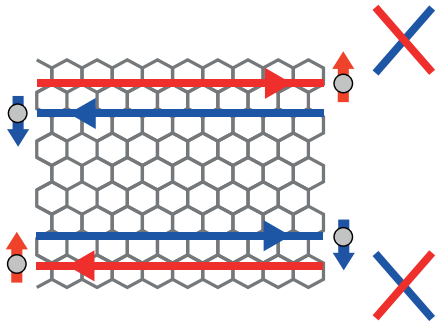

- However, SOC is too weak in graphene (E_g = 25 μeV)
- QSHE predicted and observed in HgTe/CdTe QWs

Bernevig *et al.* '06
Koenig *et al.*, '07

QSHE in HgTe quantum wells

2006: Prediction of quantum spin Hall effect in HgTe/CdTe QWs

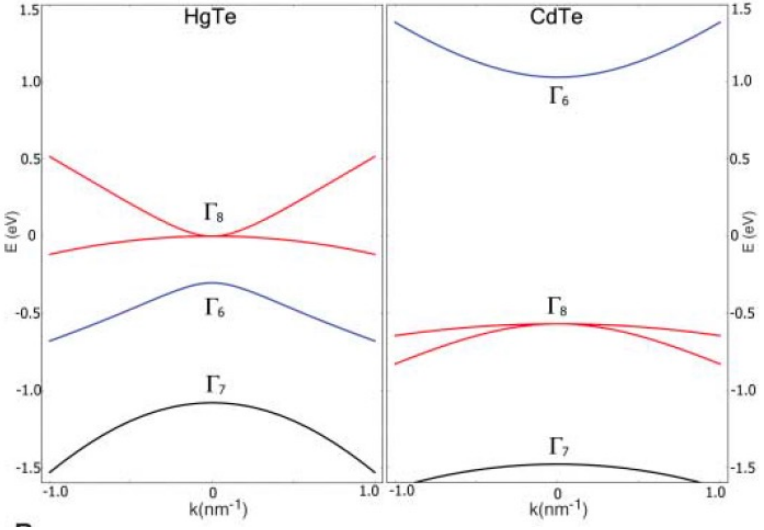

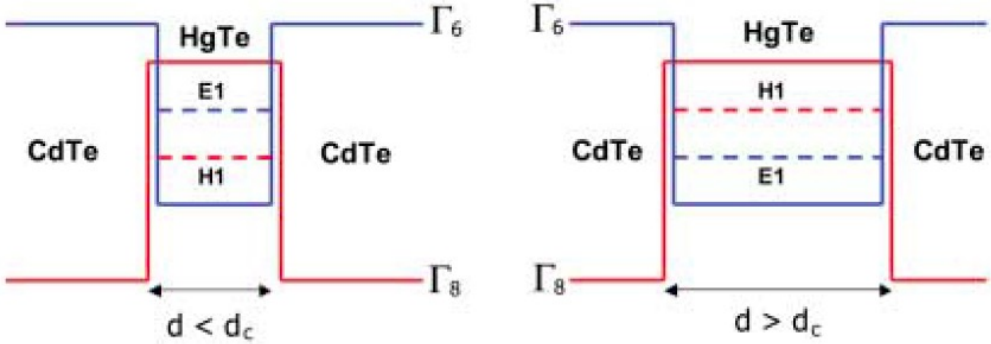

Bernevig *et al.*, Science **314**, 1757 (2006)

2007: Experimental confirmation (transport)

$$G = \frac{2e^2}{h}$$

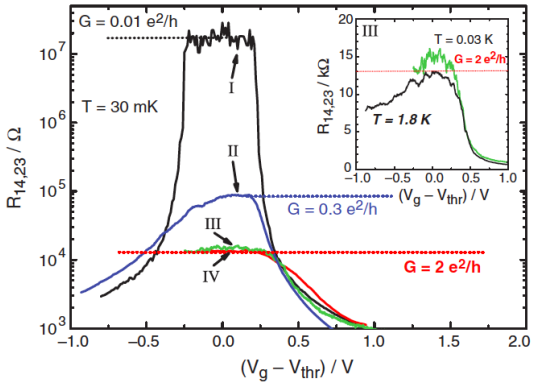

Koenig *et al.*, Science **318**, 766 (2007)

Z_2 topological insulators

- Z_2 invariant ν (with inversion symmetry)

$$(-1)^{\nu} = \prod_{a=1}^{2^d} \delta_a \qquad \delta_a = \prod_m \xi_m(\Lambda_a)$$

Λ_a - time-reversal invariant momentum (TRIM) points

ξ_m - wavefunction parity

TRIM points in 2D

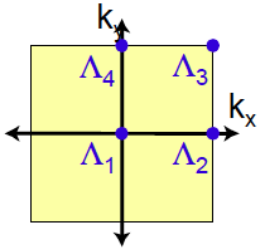

Fu and Kane (2007)

- Basic topological insulator (TI) recipe:
  - Band inversion involving states of different parity
  - Band gap open by spin-orbit interactions

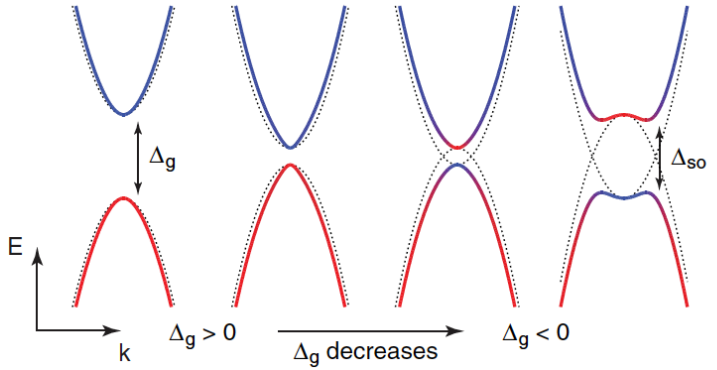

Z2Pack approach

Hybrid Wannier function: wannierisation along one direction only:

$$|R_x k_y n\rangle = \frac{1}{2\pi}\int e^{-iR_x k_x}|\psi^{n,\vec{k}}\rangle \mathrm{d}k_x$$

The Hybrid Wannier charge center...

$$\bar{x}(k_y) = \langle 0 k_y n|x|0 k_y n\rangle$$

... is directly related to the Berry connection

$$\bar{x}(k_y) = \frac{ia_x}{2\pi}\int \langle u_{nk}|\partial_{k_x}|u_{nk}\rangle \mathrm{d}k_x = \frac{a_x}{2\pi}\int \mathcal{A}_x(k_y)\mathrm{d}k_x$$

Chern number

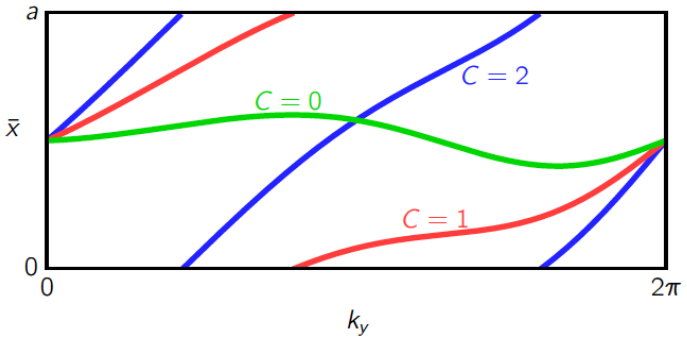

Z_2 index

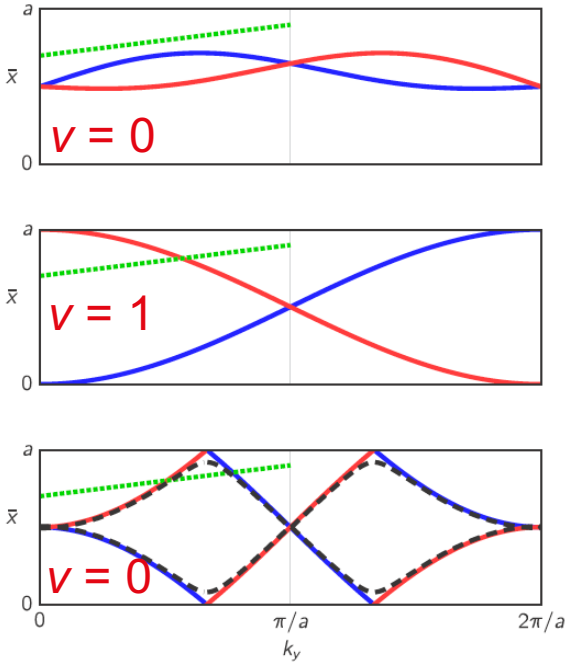

Soluyanov & Vanderbilt, PRB'11, PRB'12
Gresch *et al.*, PRB 95, 075146 (2017)

Z_2 topological insulators

- 2D TI - quantum spin Hall insulator

  ν (= 0 or 1)

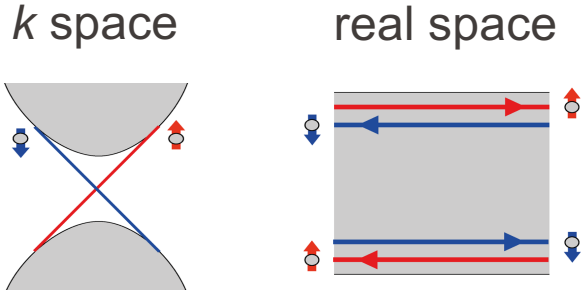

- 3D TI – crystalline materials

  $(\nu_0; \nu_1\nu_2\nu_3)$ – 16 topological classes

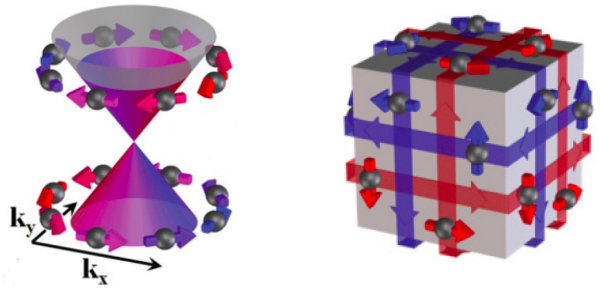

- consequences:
  - suppressed backscattering of charge carriers
  - charge current ⇔ spin polarization

First materials realizations of bulk TIs

- similar structural motifs – Bi or Sb layered materials
- band gaps upto *ca.* 0.3 eV
- TI phase confirmed by observing surface states using ARPES
- similar surface-state dispersion – single Dirac cone at Γ

- Bi_2Se_3, Bi_2Te_3

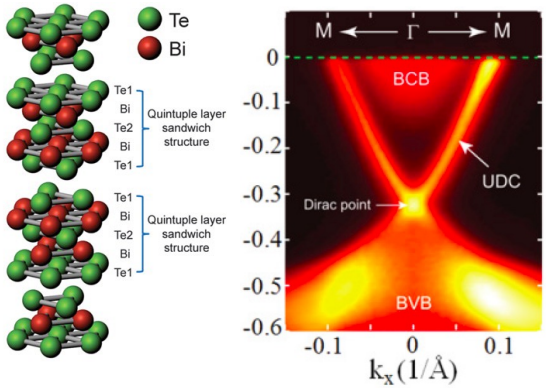

Xia *et al.*, Nature Phys. **5**, 398 (2009);
Zhang *et al.*, *ibid*. (2009)
figs from Chen *et al.*, Science'09

- $TlBiSe_2$

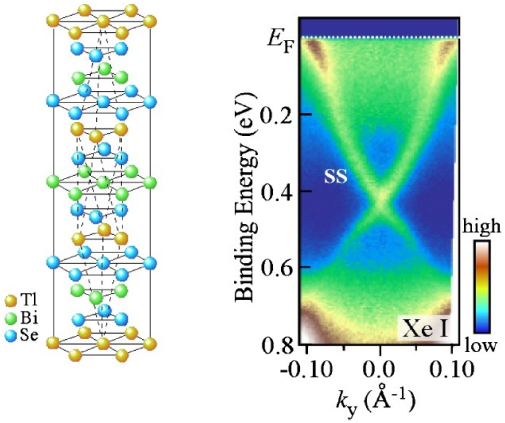

Sato *et al.*, PRL **105**, 136802 (2010)

- $PbBi_4Te_7$

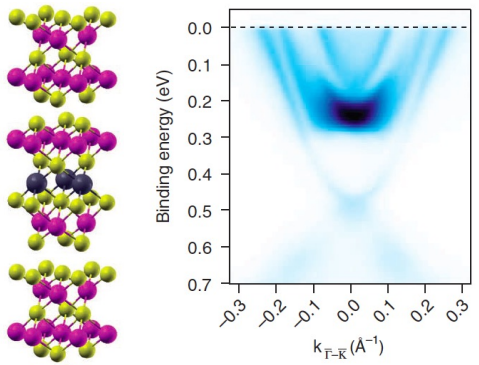

Eremeev *et al.*, Nat. Commun'12

Spin-orbit interactions across periodic table

- spin-orbit coupling $\mathbf{H}_{\mathrm{SO}} = \zeta \mathbf{L} \cdot \mathbf{S}$ is a relativistic effect
- in neutral atoms $\zeta \propto Z^2$ across the vertical direction of PT
  (and not $\zeta \propto Z^4$ as often quoted, but the truth can be found in Landau-Lifshitz, as usual)
- faster growth across the horizontal dimension
- standard DFT calculations provide quantitative description

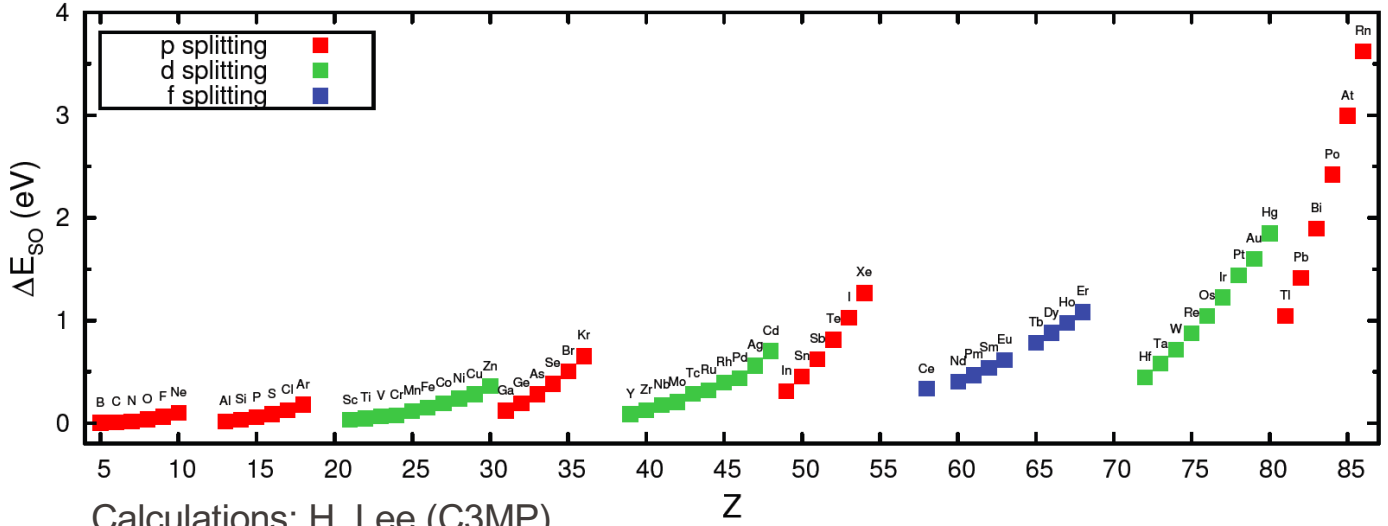

Calculations: H. Lee (C3MP)

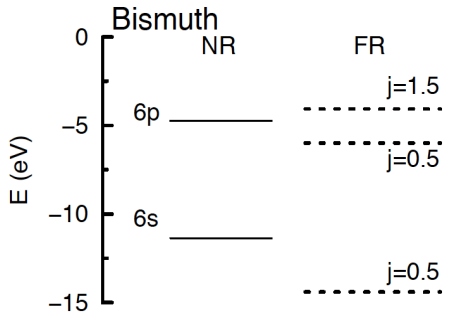

$$E_{6p}^{j=3/2} - E_{6p}^{j=1/2} = \frac{3}{2}\zeta_{6p} = 1.9\,\mathrm{eV}$$

Electronic structure of Bi chalcogenides

- band inversion results from competing spin-orbit and ligand/crystal field splitting
- spin-orbit coupling is inherited from atoms
- spin-orbit coupling defines the band gap
- a simple model provides quantitative description

- Bi_2Se_3

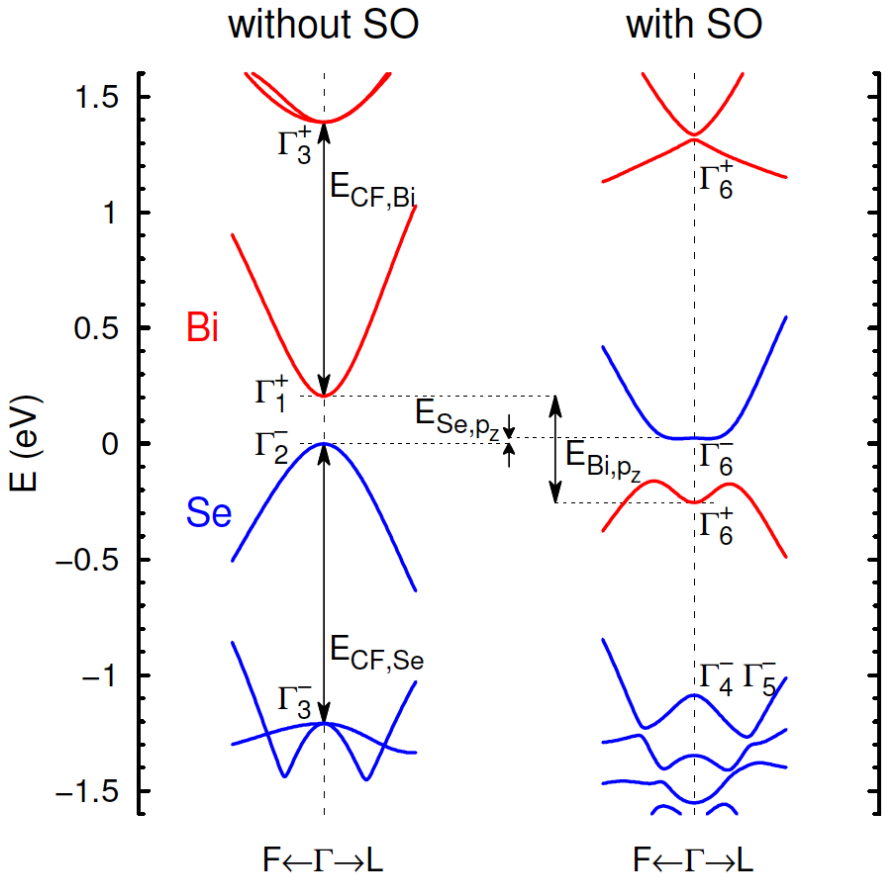

H. Lee and O. V. Yazyev, JPCM **27**, 285801 (2015)

Oleg Yazyev

Timeline of the field of topological materials

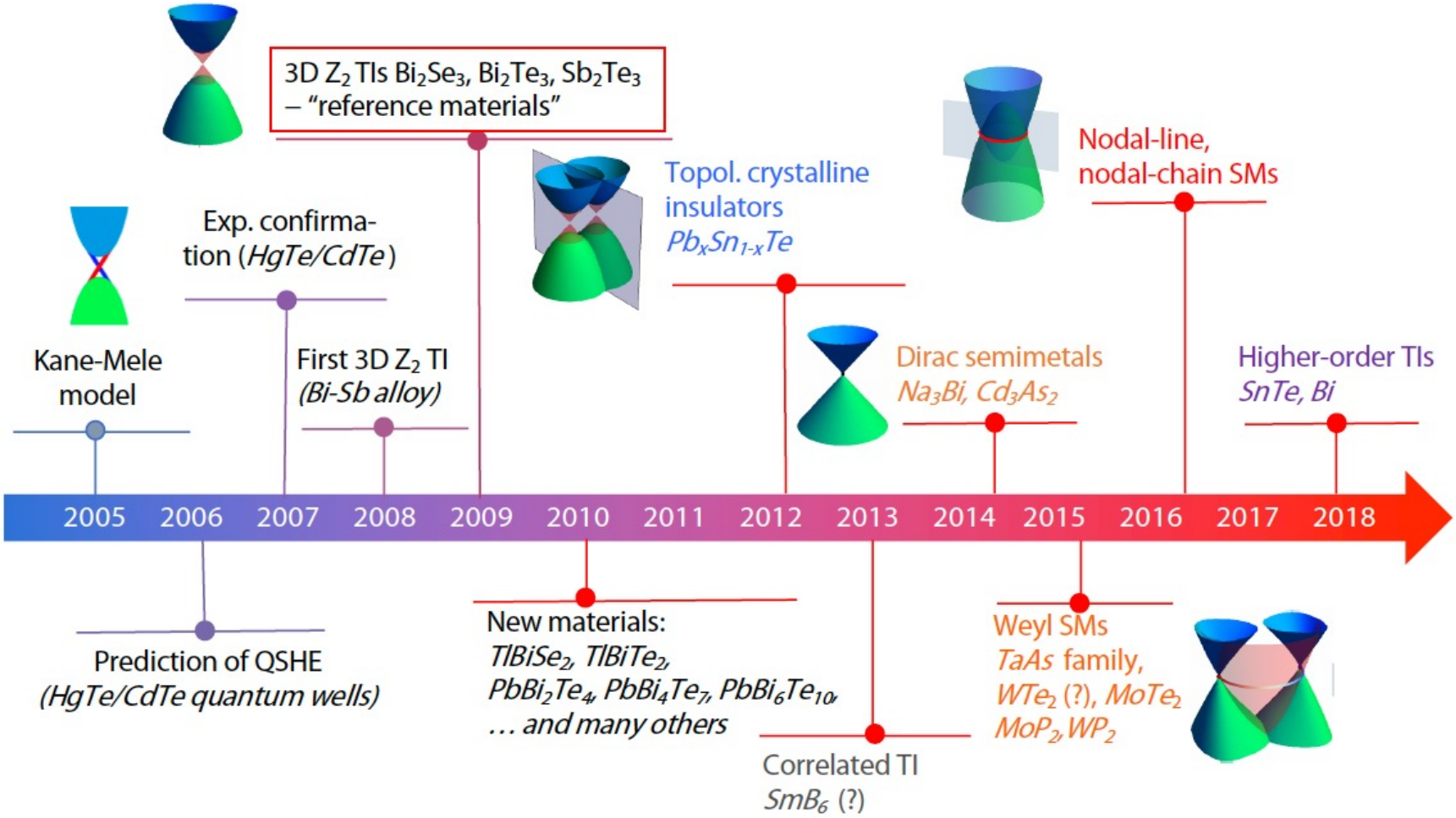

High-throughput search protocol

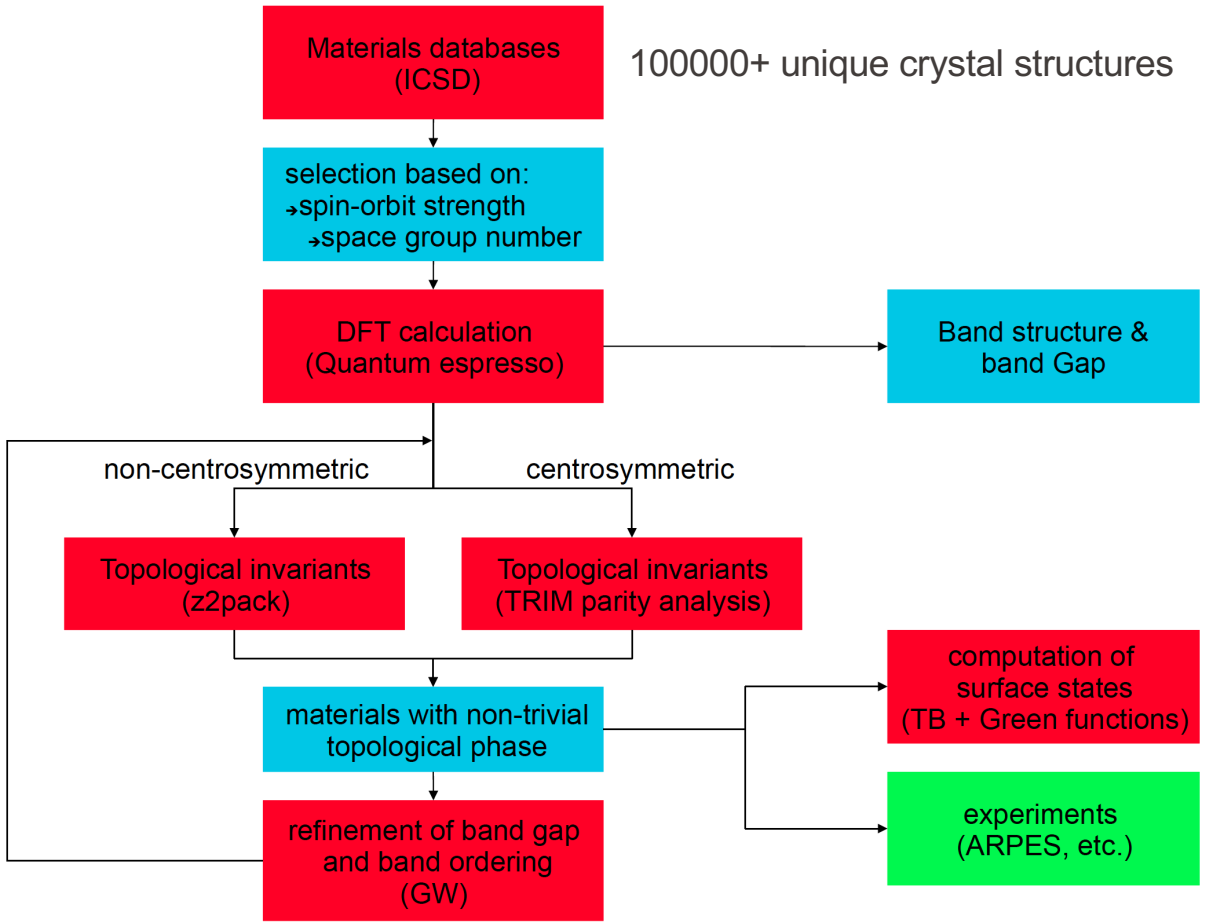

G. Autès (C3MP)

MARVEL MATERIALS REVOLUTION

NCCR Marvel

European Research Council erc

ERC Starting grant TopoMat

TopoMat database @ Materials Cloud

- started in 2013, made publicly available in 2018
- crystal structures from ICSD and COD databases (experimental XRD data) – total 108423 unique crystal structures
- currently 13628 entries (“pre-screened” materials: <20 atoms per unit cell, even number of electrons, no lanthanides)
- band structures, Z_2 indices, Wannier charge center plots (Z2Pack), etc.
- >4000 materials with nontrivial Z_2 indices
- all data is freely available on Materials Cloud

doi: 10.24435/materialscloud:2019.0019/v2

TopoMat: a database of high-throughput first-principles calculations of topological materials

DOI 10.24435/materialscloud:2019.0019/v1

Authors: Gabriel Autès, QuanSheng Wu, Nicolas Mounet & Oleg V. Yazyev

Description: The database contains the results of high-throughput first-principles screening of known crystal structures for topological materials (topological insulators, Dirac and Weyl semimetals, etc.). If you use this work please cite the following publication in progress: G. Autès, Q. S. Wu, N. Mounet & O. V. Yazyev, “TopoMat: a database of high-throughput first-principles calculations of topological materials”, in preparation (2018).

Oleg Yazyev

TopoMat database @ Materials Cloud

- web interface and search engine on Materials Cloud
  https://www.materialscloud.org/discover/topomat

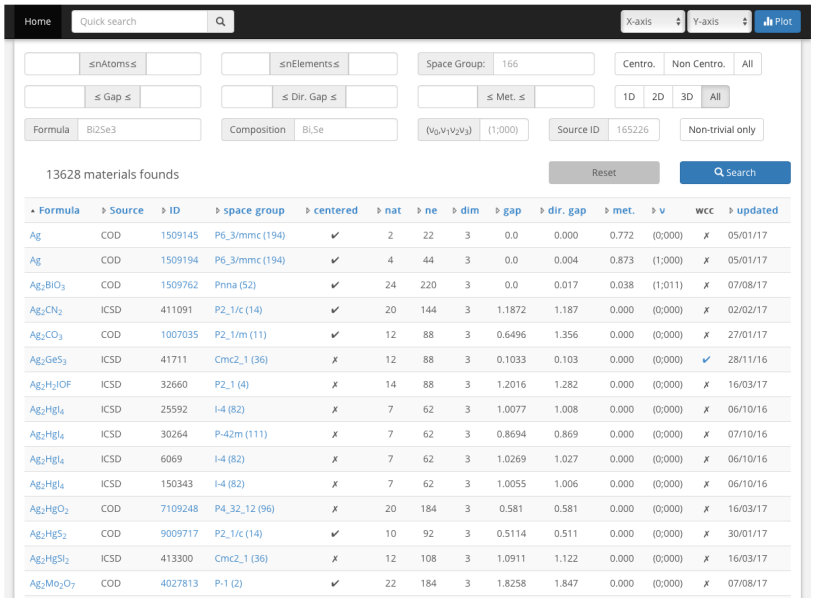

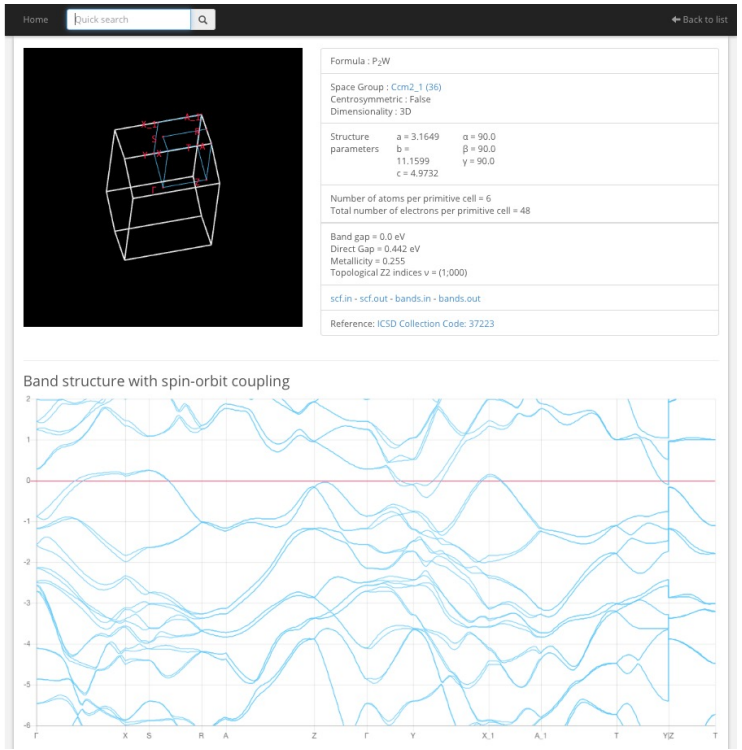

β-Bi_4I_4 – a «candidate» topological insulator

- quasi-1D crystal structure (space group C12/m1)

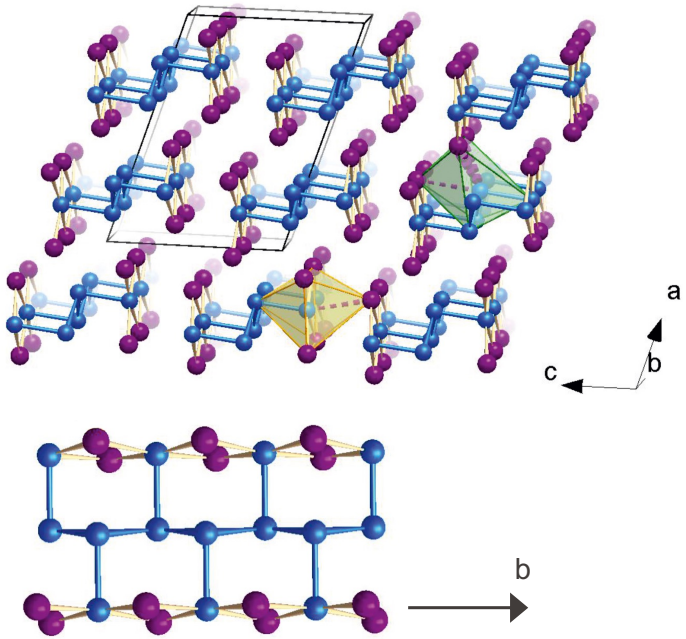

Urazov & Sokolova, 1954
von Schnering *et al.*, 1978

- DFT predictions
  - band gap 0.14 eV
  - «weak» TI (0;001)
  - band inversion at points M and Y

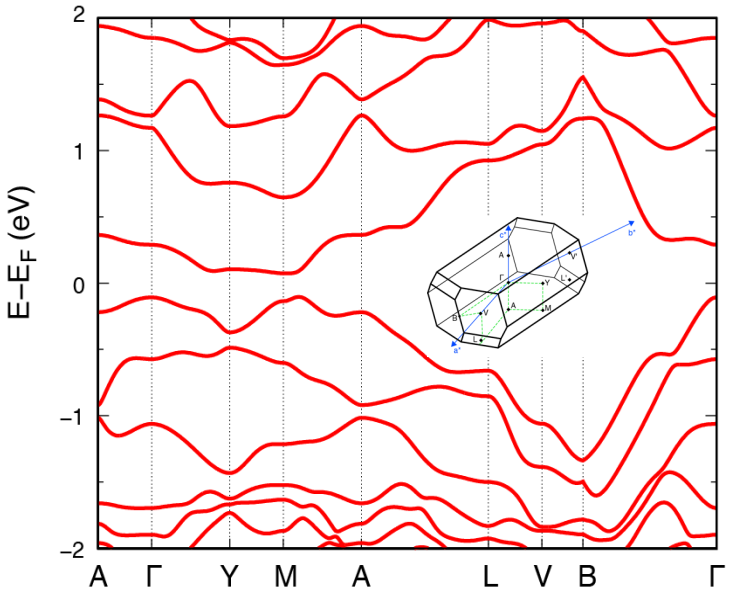

Oleg Yazyev

β-Bi_4I_4 – signatures of the topological phase

- weak 3D TI = stack of 2D TIs

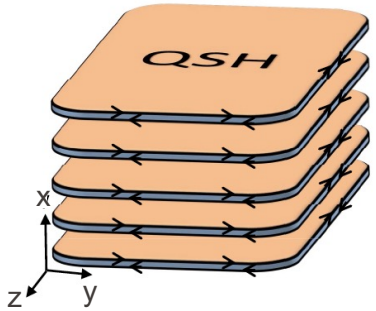

- surface-state dispersion at side surfaces = Dirac "groove"

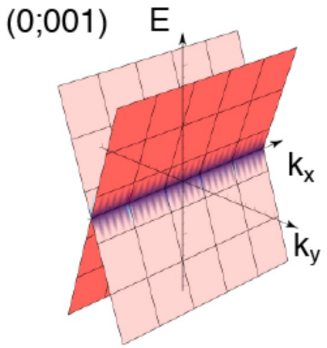

- Predicted dispersion:
  - (001) surface

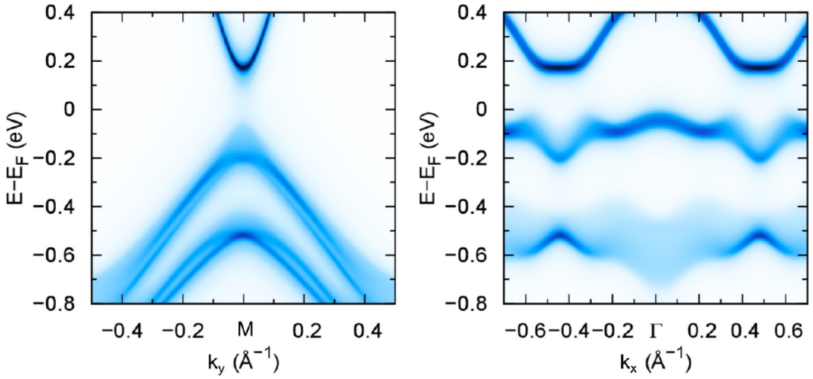

  - (100) surface

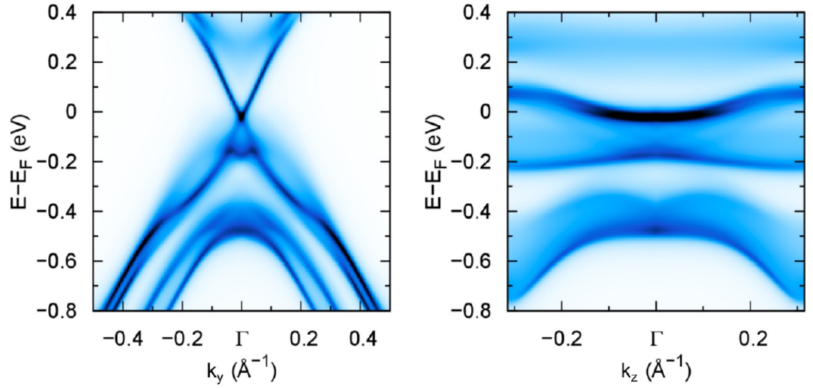

C3MP

Chair of Computational Condensed Matter Physics

β-Bi_4I_4 – synthesis and characterization

- synthesis

A. Isaeva (TU Dresden)

- TEM characterization

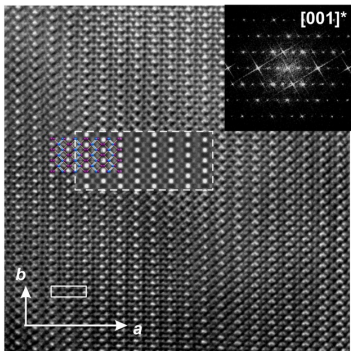

W. van den Broek (Ulm)

- transport measurements

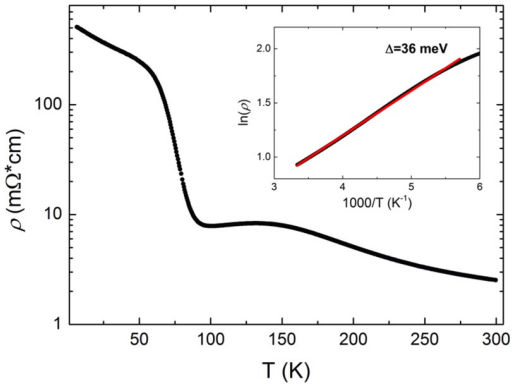

A. Pisoni, L. Forro (EPFL)

β-Bi_4I_4 – ARPES measurements

- A clean band crossing

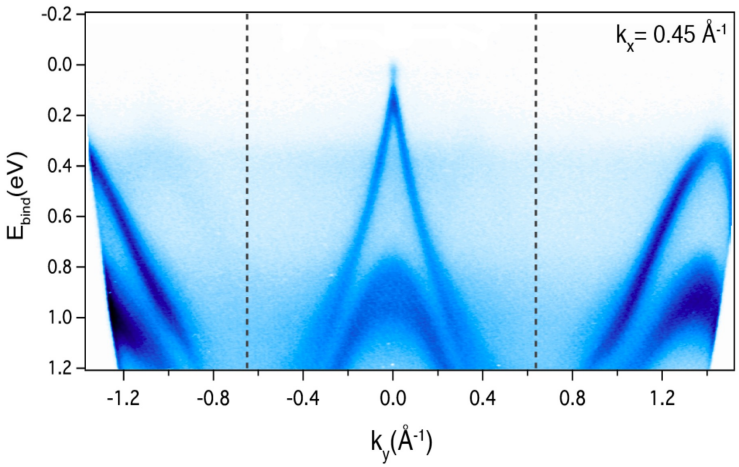

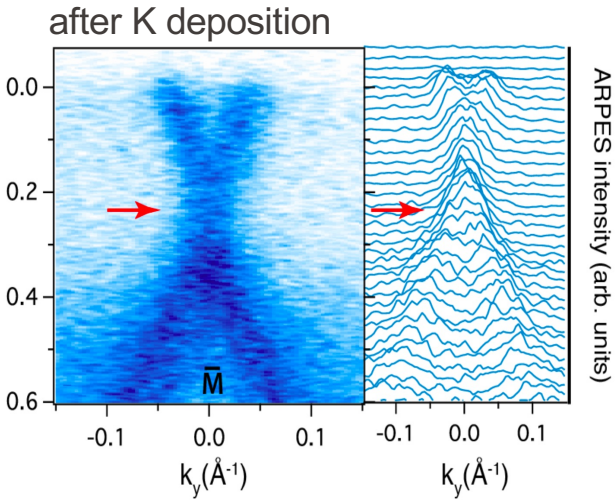

L. Moreschini (ALS)

J. Johannsen (EPFL)
M. Grioni (EPFL)

- … but at (001) surface, and anisotropic Dirac cone

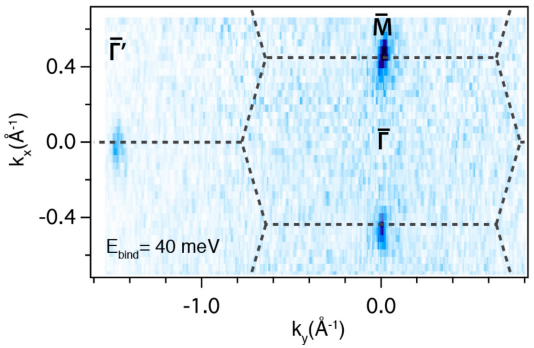

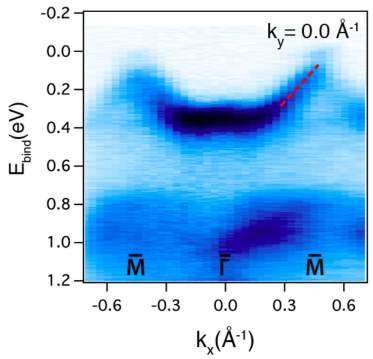

First-principles calculations (DFT vs. MBPT)

- Density functional theory (DFT)
  - Kohn-Sham formalism

$$\left[-\frac{1}{2}\nabla^2 + V_{\text{ion}} + V_{\text{H}} + V_{\text{xc}}^{\text{DFT}}\right]\psi_{n\mathbf{k}}^{\text{DFT}} = E_{n\mathbf{k}}^{\text{DFT}}\psi_{n\mathbf{k}}^{\text{DFT}}$$

Hohenberg & Kohn '64
Kohn & Sham '65

  - Good for: ground-state properties (structural, cohesive, vibrational, magnetic, …)
  - Bad for: excited-state properties (photoemission, band gaps, band offsets, optical, ...)

- Many-body perturbation theory (MBPT)
  - *GW* formalism: Green's function approach + quasiparticle approximation

$$\left[-\frac{1}{2}\nabla^2 + V_{\text{ion}} + V_{\text{H}} + \Sigma(E_{n\mathbf{k}}^{\text{QP}})\right]\psi_{n\mathbf{k}}^{\text{QP}} = E_{n\mathbf{k}}^{\text{QP}}\psi_{n\mathbf{k}}^{\text{QP}}$$

Hedin '65
Hybertsen & Louie '85

$\Sigma = iGW$ - self energy

G - one-particle Green's function

$W = \varepsilon^{-1}\upsilon$ - screened Coulomb interaction

The band-gap problem

- DFT vs. GW results

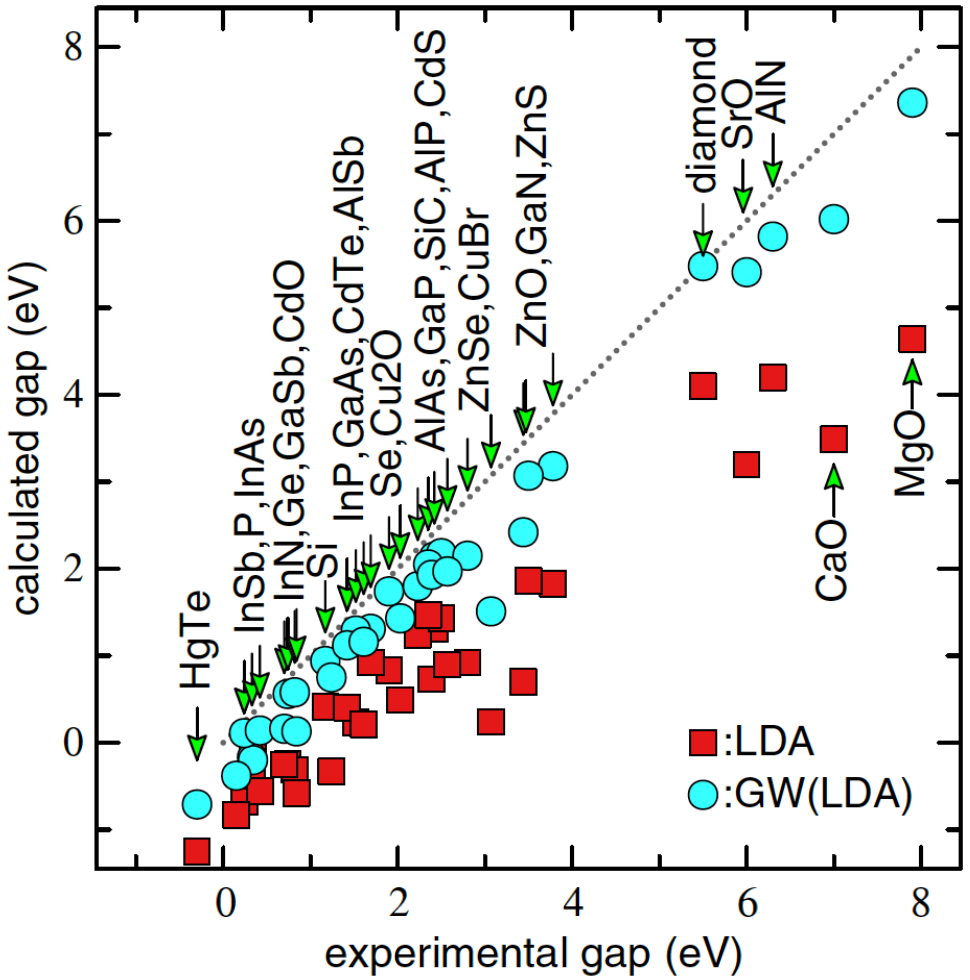

From van Schilfgaarde *et al.*,
Phys. Rev. Lett. **96**, 226402 (2006)

β-Bi_4I_4 : the «revised» predictions (GW)

- DFT "exaggerates" band inversion (Yazyev *et al.*, PRB'12)
- GW corrections eliminate band inversion at point M

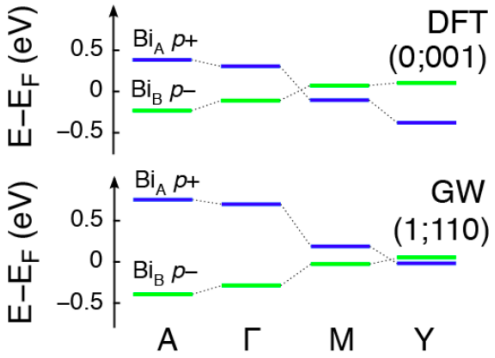

- ~~"weak" topological insulator (0;001)~~
- "strong" topological insulator (1;110)
- band gap 0.037 eV

- Simulated ARPES at the (001) surface

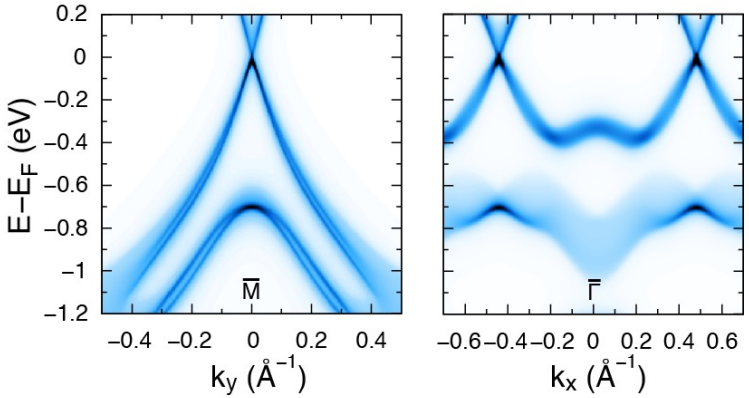

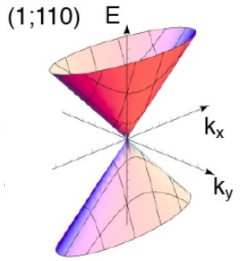

anisotropic Dirac fermions

G. Autès *et al.*, Nature Materials **15**, 154 (2016)

β-Bi_4I_4 : possible phases

- Rigid quasiparticle shift before introducing spin-orbit interactions

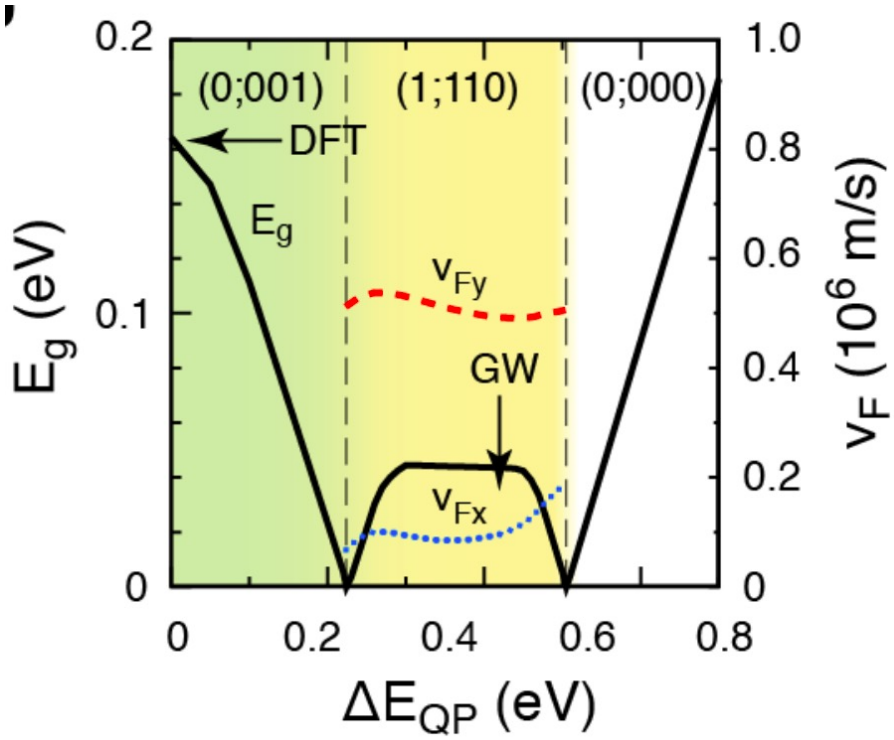

G. Autès *et al.*, Nature Materials **15**, 154 (2016)

β-Bi_4I_4 : theory vs. experiment

- Theory (*GW*)

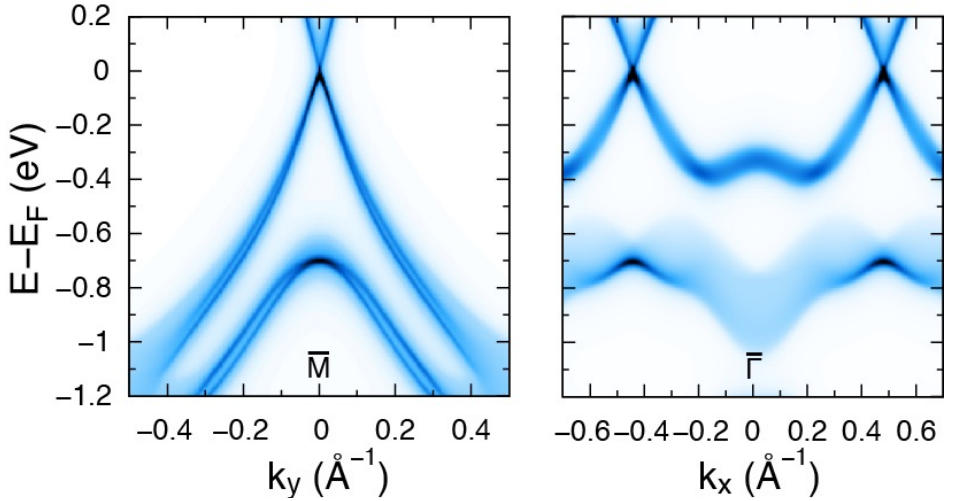

- close view (bulk/surface)

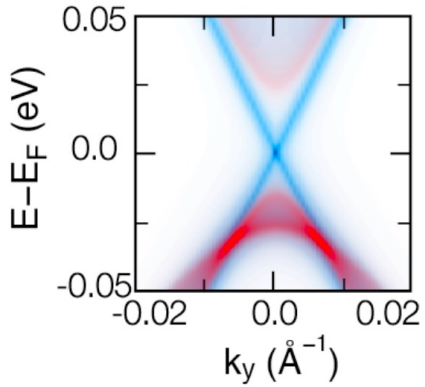

- Experiment

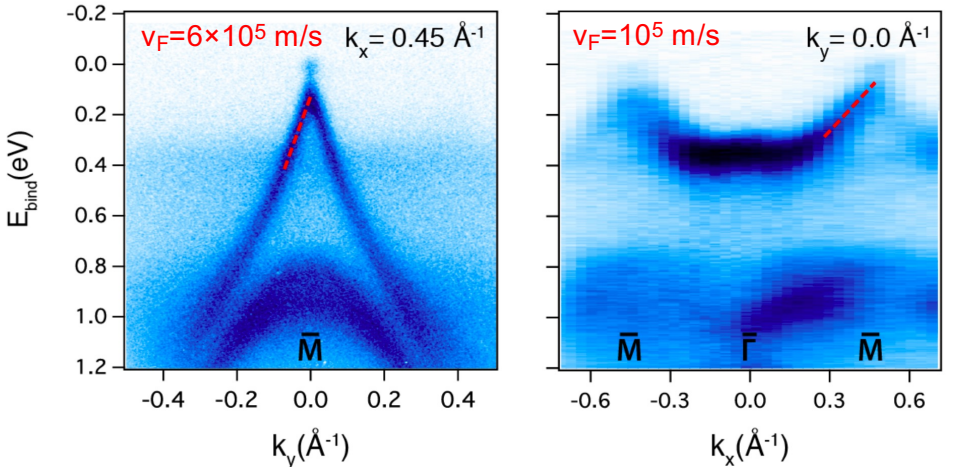

- 6 eV laser ARPES

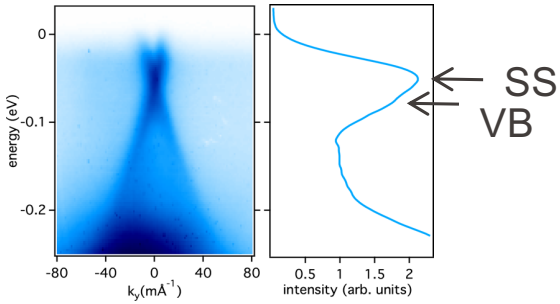

G. Autès *et al.*, Nature Materials **15**, 154 (2016)

β-Bi_4I_4 : theory + experiment

- Full cycle of material discovery =
  prediction, synthesis, characterization, confirmation

LETTERS
PUBLISHED ONLINE: 14 DECEMBER 2015 | DOI: 10.1038/NMAT4488
nature materials

A novel quasi-one-dimensional topological insulator in bismuth iodide β-Bi_4I_4

Gabriel Autès[1,2†], Anna Isaeva[3†], Luca Moreschini[4†], Jens C. Johannsen[5†], Andrea Pisoni[5], Ryo Mori[6,7], Wentao Zhang[6,8], Taisia G. Filatova[9], Alexey N. Kuznetsov[9], László Forró[5], Wouter Van den Broek[10], Yeongkwan Kim[4,11], Keun Su Kim[12,13], Alessandra Lanzara[6,8], Jonathan D. Denlinger[4], Eli Rotenberg[4], Aaron Bostwick[4], Marco Grioni[5] and Oleg V. Yazyev[1,2*]

- theory (Lausanne)
- materials synthesis (Dresden, Moscow)
- synchrotron ARPES (Berkeley, Lausanne, Seoul)
- 6 eV laser ARPES (Berkeley)
- transport characterization (Lausanne)
- TEM characterization (Ulm)

G. Autès *et al.*, Nature Materials **15**, 154 (2016)

β-Bi_4I_4: conclusions and outlook

- β-Bi_4I_4 is a new strong TI, very different from other known TIs
- quasi-1D structure and anisotropic Dirac fermion surface states
- very few defects and low concentration of intrinsic charge carriers
- close to the topological phase transitions to the “weak” TI (0;001) and trivial (0;000) phases, “weak” TI claimed by some groups recently
- opens an entirely new class of Bi halide topological materials (ongoing)
- higher-order topological and QSH (in thin films) insulators found by other groups

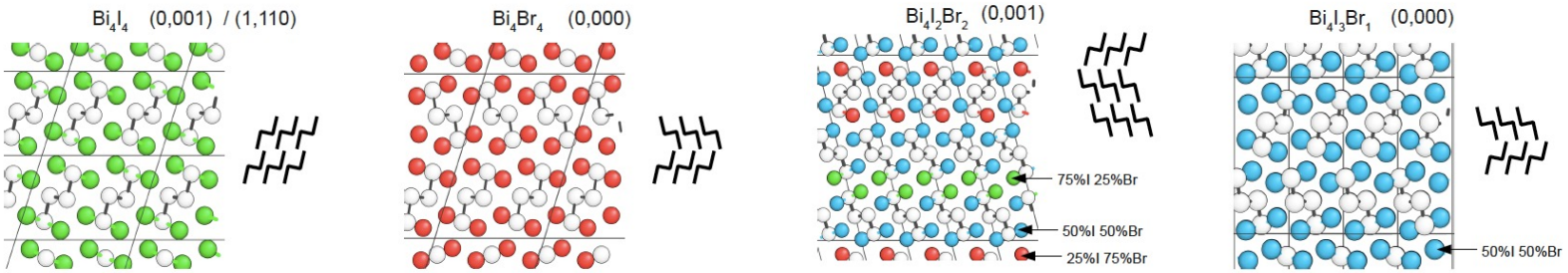

Weyl semimetals

- chiral point degeneracies (Weyl fermions)
- required breaking inversion or time-reversal symmetry
- Fermi arc surface states
- anomalous magnetotransport (chiral anomaly)

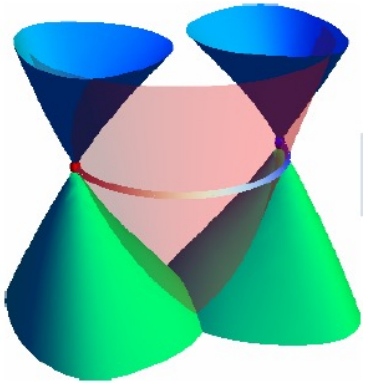

Type I

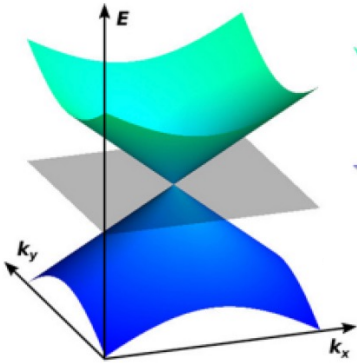

TaAs, NbAs, TaP, NbP

Lv *et al.*, 2015

Type II

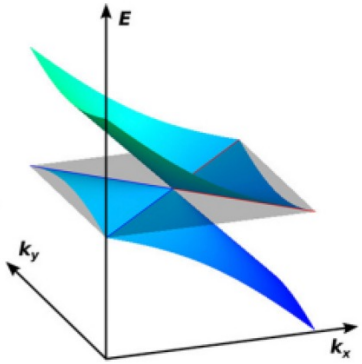

WTe_2 (?), $MoTe_2$

A. Soluyanov *et al.*, Nature 527, 495 (2015)

A. Soluyanov

1982 – 2019

Candidate Weyl semimetals MoP_2 and WP_2

- base-centered orthorhombic crystal structure
- space group $Cmc2_1$ (No. 36)
- symmetries:
  - C_2 screw axis along [001]
  - mirror plane (010)
  - glide plane (100)

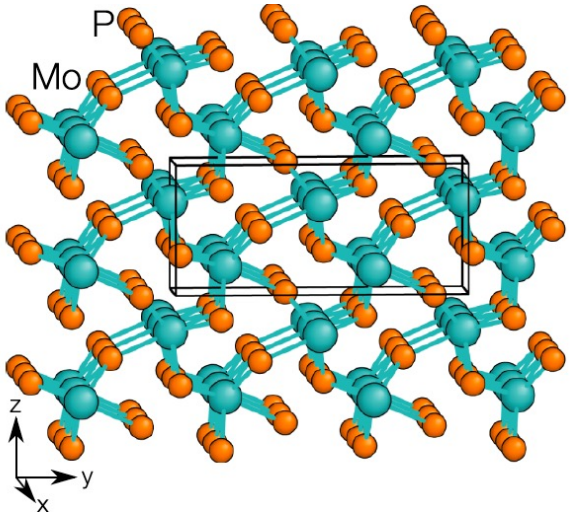

Rundqvist and Lundström ’63
Rühl and Jeitschko ‘83

- compensated semimetals
- very similar band structures

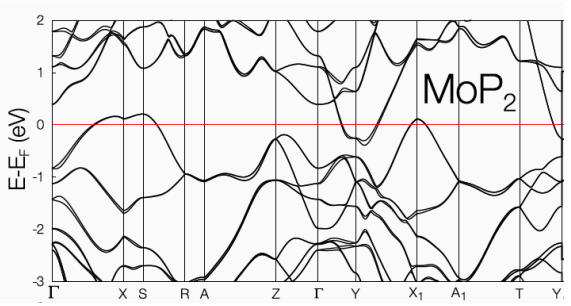

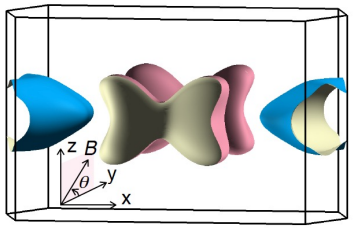

Fermi surface

Autès *et al.*, Phys. Rev. Lett. **117**, 066402 (2016)

Oleg Yazyev

Candidate Weyl semimetals MoP_2 and WP_2

- 8 Weyl points of type II in k_z = 0 plane

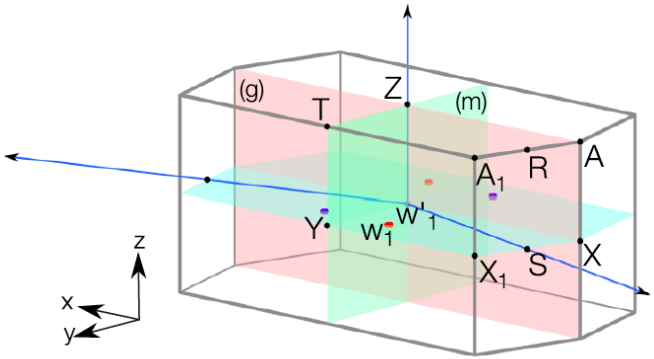

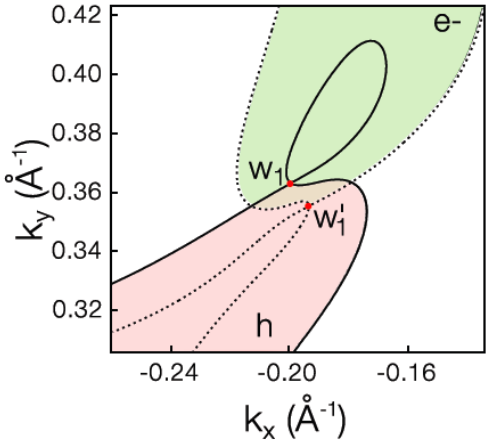

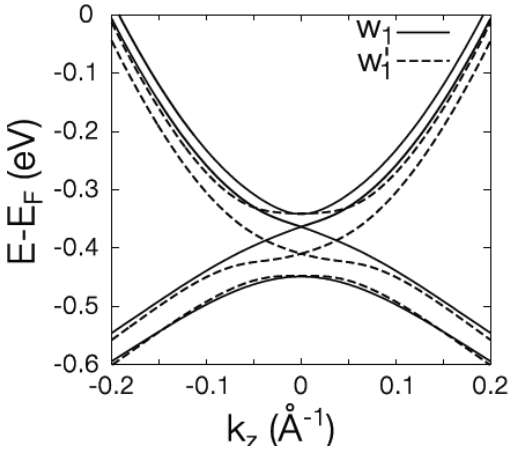

- Robust Weyl semimetal phase
  - large distance in *k* space between Weyl points of opposite chirality

TaAs family: ~4% of reciprocal lattice vector;
WTe_2 family ~1%
MoP_2 and WP_2 **~25%**

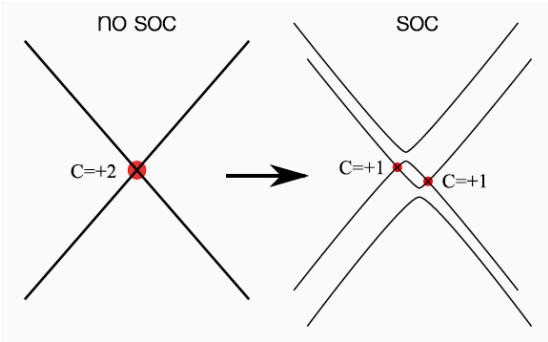

Autès *et al.*, Phys. Rev. Lett. **117**, 066402 (2016)

C3MP
Chair of Computational Condensed Matter Physics

Candidate Weyl semimetals MoP_2 and WP_2

- Long Fermi arcs that depend on surface termination

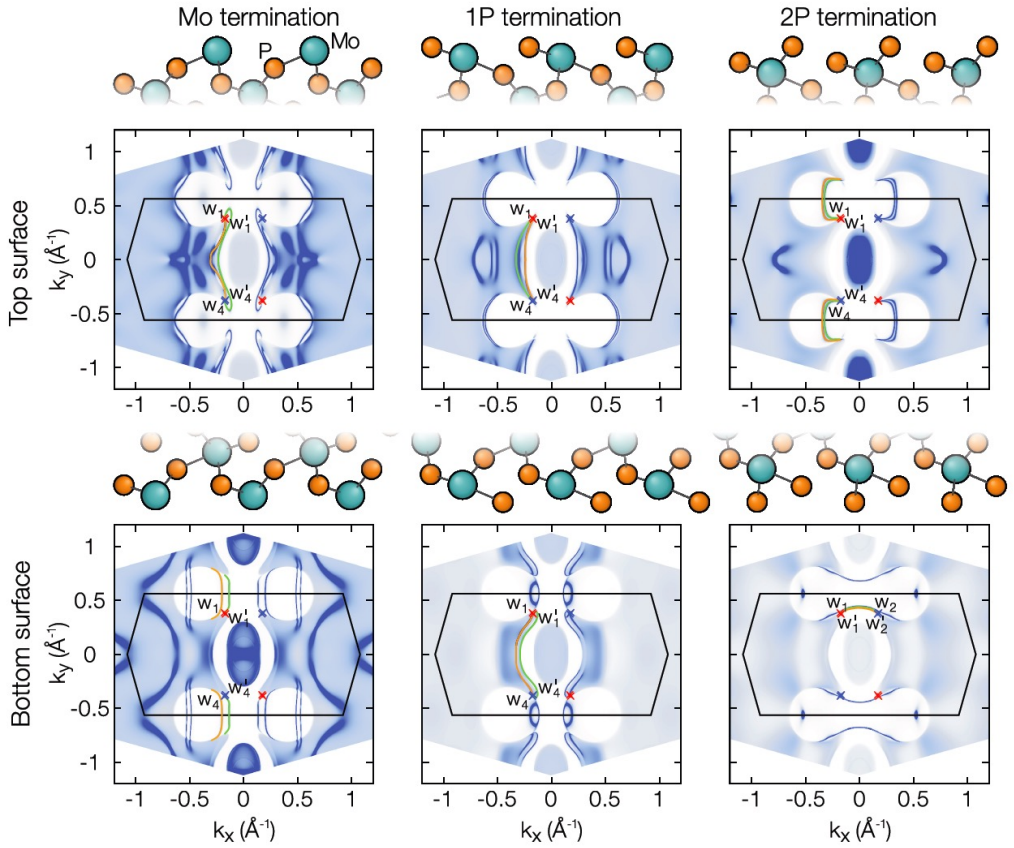

Autès *et al.*, Phys. Rev. Lett. **117**, 066402 (2016)

Oleg Yazyev

C3MP
Chair of Computational Condensed Matter Physics

Early experimental results

- very high low-T conductivity ($\rho \approx 3$ nΩ cm at 2 K)
- residual resistivity ratios (RRR ≈ 25000) record for binary materials
- highest measured magnetoresistances (2×10^8 % at 63 T and 0.5 K, 4×10^6 % at 9 T and 2 K)
- mean free path of 0.5 mm

  N. Kumar *et al.*, Nat. Commun. 8, 1642 (2017)

- hydrodynamic electron fluid transport below 20 K

  J. Gooth *et al.*, Nat. Commun. 9, 4093 (2018)

- "negative" resistivity (at low T and for B||E)

  Y.-Y. Lv *et al.*, arXiv:1708.03489

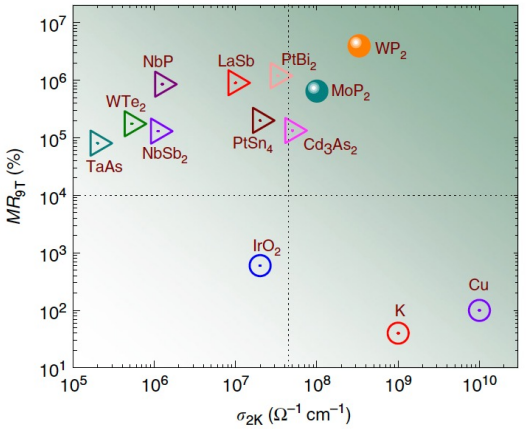

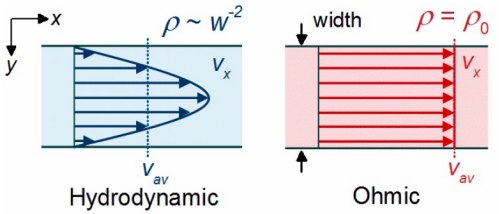

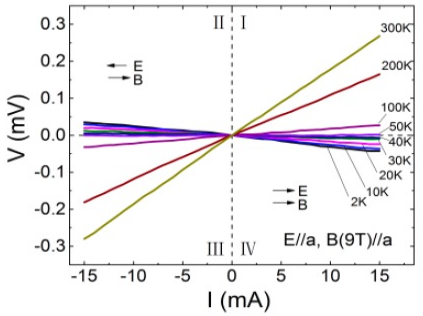

ARPES confirmation of Weyl nodes in WP_2

- Very good agreement with DFT calculations

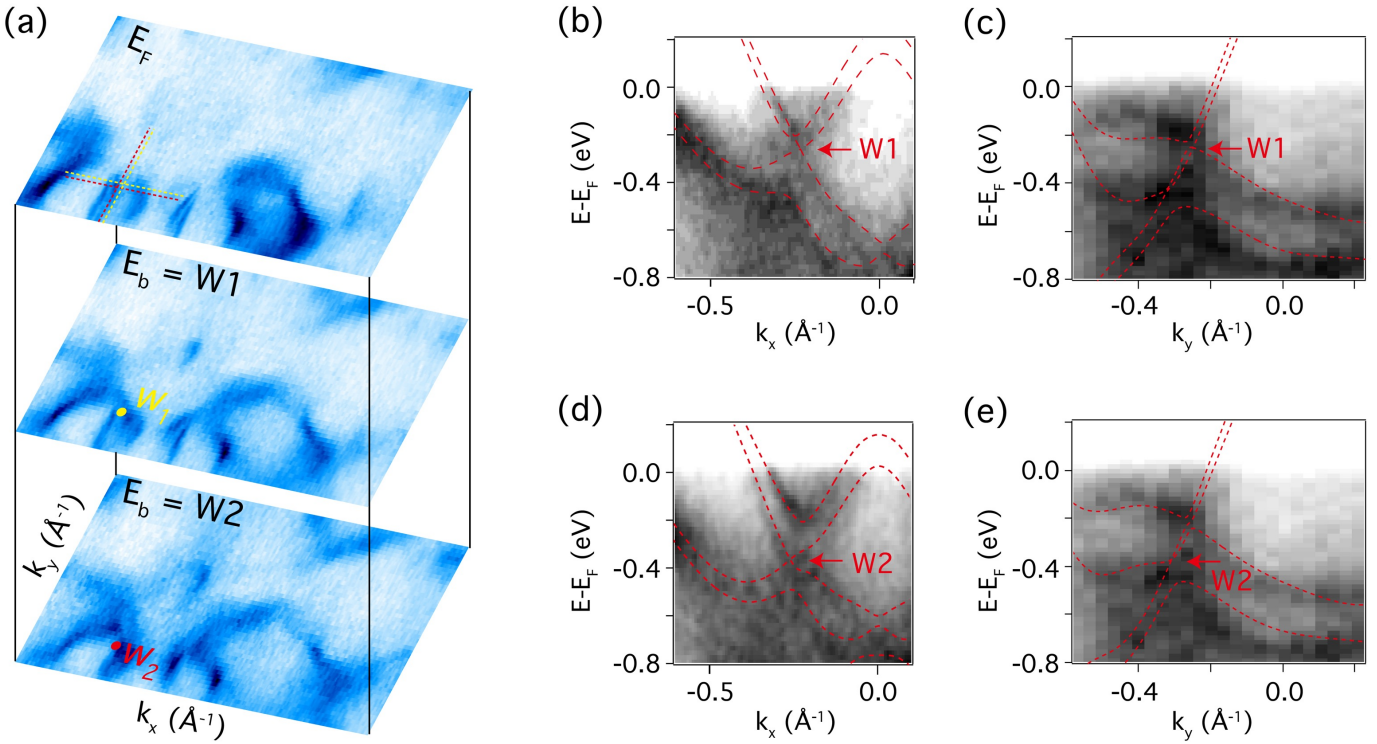

ARPES:
group M. Shi (PSI)

M.-Y. Yao *et al.*, Phys. Rev. Lett. 122, 176402 (2019)

Transverse magnetoresistance in WP_2

Magnetoresistance $$\mathrm{MR}(B) = \frac{\rho(B) - \rho(0)}{\rho(0)}$$

- Extremely large, non-saturating, nearly quadratic MR ($I \parallel a$, $B \parallel b$)
- No sign of quantum oscillations

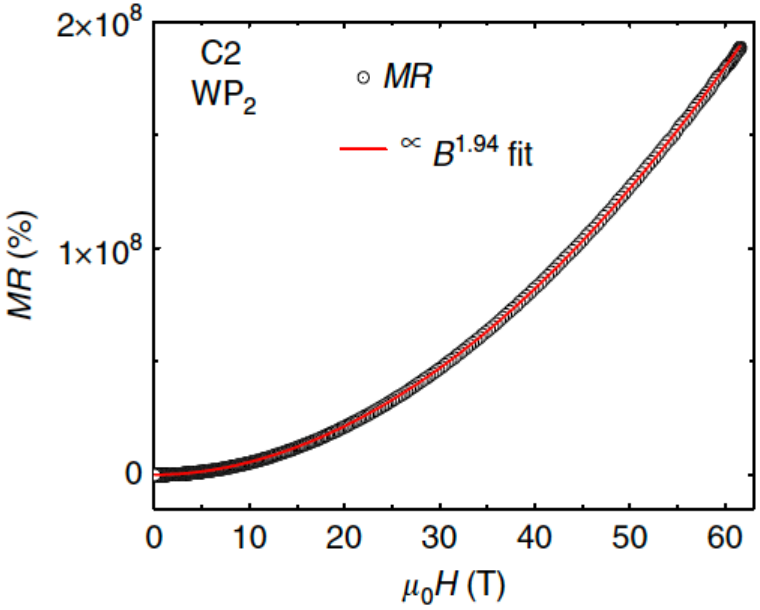

- Very pronounced MR anisotropy

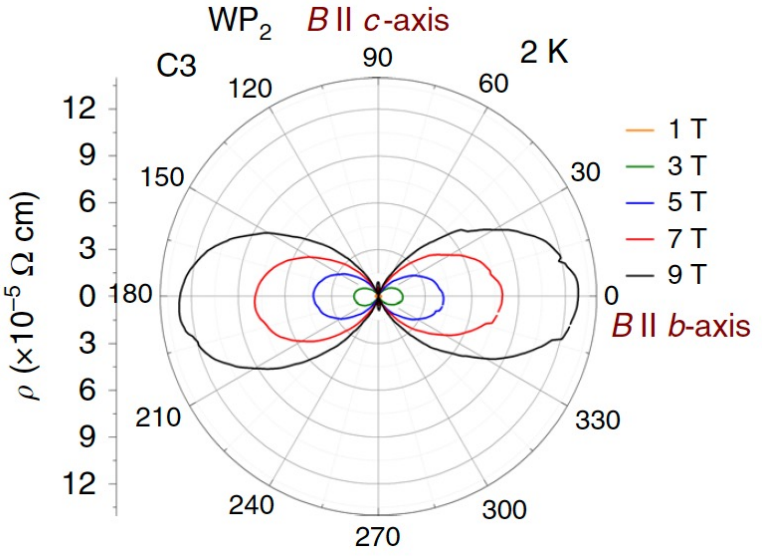

N. Kumar *et al.*, Nat. Commun. 8, 1642 (2017)

Origin of non-saturating MR

Within the semiclassical approximation:

- free electrons (spherical Fermi surface) : MR = 0
- nearly free electrons : MR $\propto B^2$, then saturates

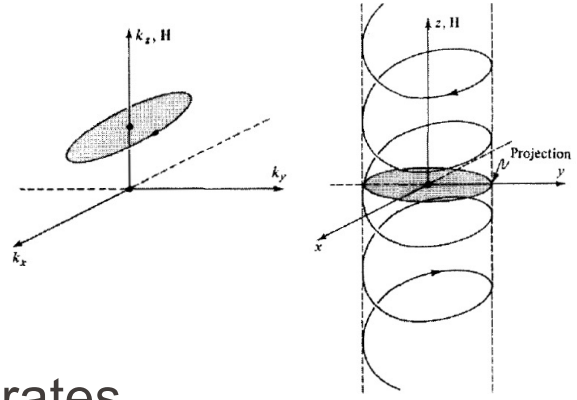

- compensated semimetal (**1**) : MR $\propto B^2$, never saturates
- nearly compensated semimetal (**2**) : MR $\propto B^n$, $n < 2$
- open orbits (**3**) : non-saturating for current along the open direction

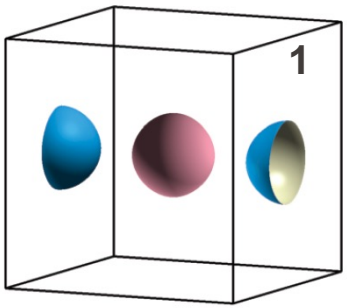

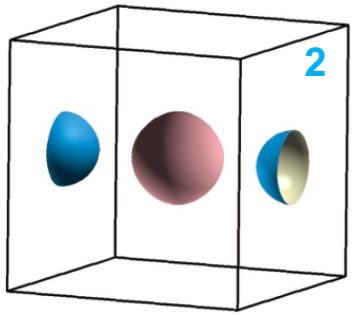

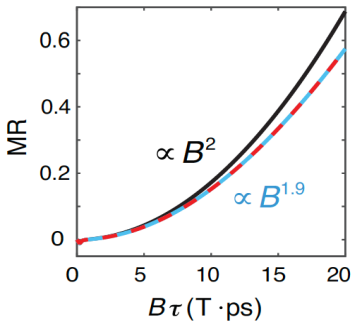

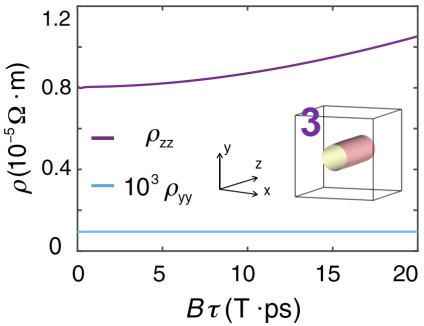

MR within semiclassical approximation

- Boltzmann transport approach

$$\sigma_{ij}^{(n)}(\mathbf{B}) = \frac{e^2}{4\pi^3}\int d\mathbf{k}\tau_n \mathbf{v}(\mathbf{k})\bar{\mathbf{v}}(\mathbf{k})\left(-\frac{\partial f}{\partial \varepsilon}\right)_{\varepsilon=\varepsilon_n(\mathbf{k})}$$

$$\mathbf{v}_n(\mathbf{k}) = \frac{1}{\hbar}\nabla_{\mathbf{k}}\varepsilon_n(\mathbf{k}) \qquad \frac{d\mathbf{k}_n(t)}{dt} = -\frac{e}{\hbar}\mathbf{v}_n[\mathbf{k}(t)]\times\mathbf{B}$$

$$\bar{\mathbf{v}}_n(\mathbf{k}) = \int_{-\infty}^{0}\frac{dt}{\tau_n}e^{\frac{t}{\tau_n}}\mathbf{v}_n[\mathbf{k}(t)]$$

S.N. Zhang

Q.S. Wu

implemented in WannierTools code

S.N. Zhang, Q.S. Wu, Y. Liu, O. V. Yazyev, PRB 99, 035142 (2019)

- Combined with first-principles calculations and Wannier function techniques
- Typically, compares well to experiments, even in constant τ approximation

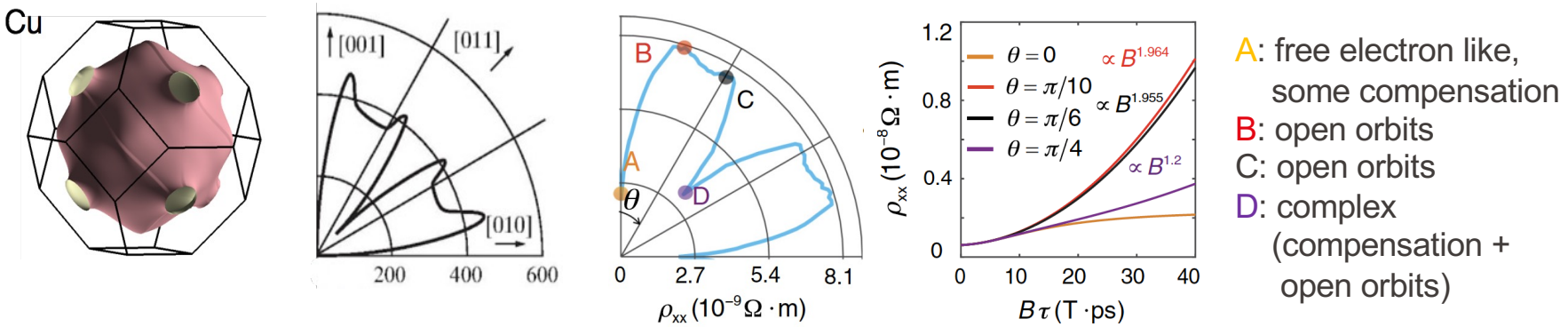

A: free electron like, some compensation
B: open orbits
C: open orbits
D: complex (compensation + open orbits)

Exp:. Klauder and Kunzler, *The Fermi Surface* (1960)

MR in WP_2 from theory perspective

- non-saturating MR results from ordinary charge carrier compensation
- not directly related to the Weyl semimetal phase, but implies a relatively long $\tau = 10^{-9}$ s

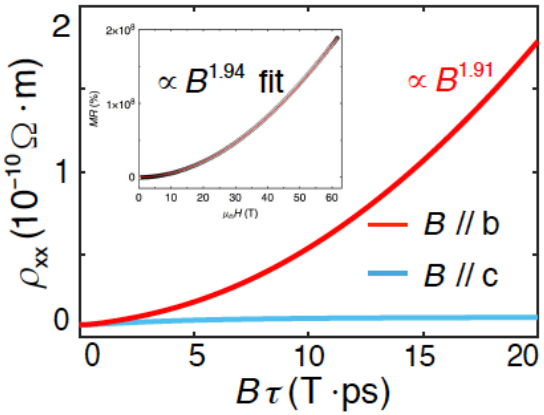

- novel mechanism for strong MR anisotropy
  - for B || c, hole carriers follow elec. orbits
  - result of concave FS segments

N.P. Ong, PRB 43, 193 (1991)

Fermi surface of WP_2

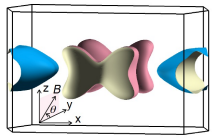

Exp:

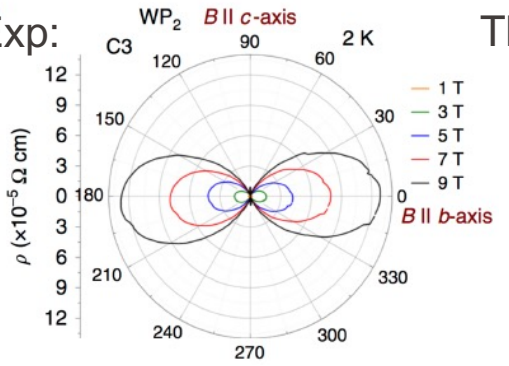

Theory:

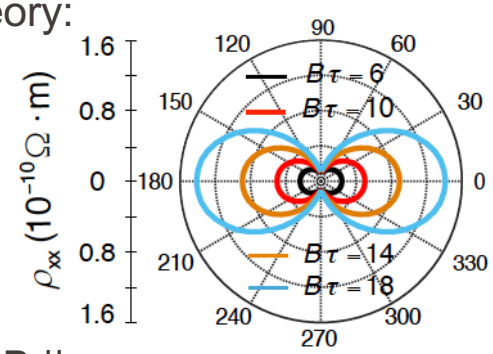

B || b

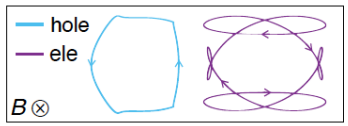

B || c

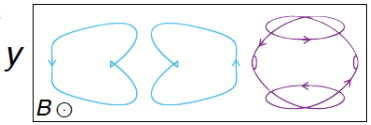

S.N. Zhang, Q.S. Wu, Y. Liu, O. V. Yazyev, PRB 99, 035142 (2019)

Band structure of ordinary bcc iron

- Numerous Weyl points across the band structure as a result of broken time-reversal symmetry

magnetization along [001]

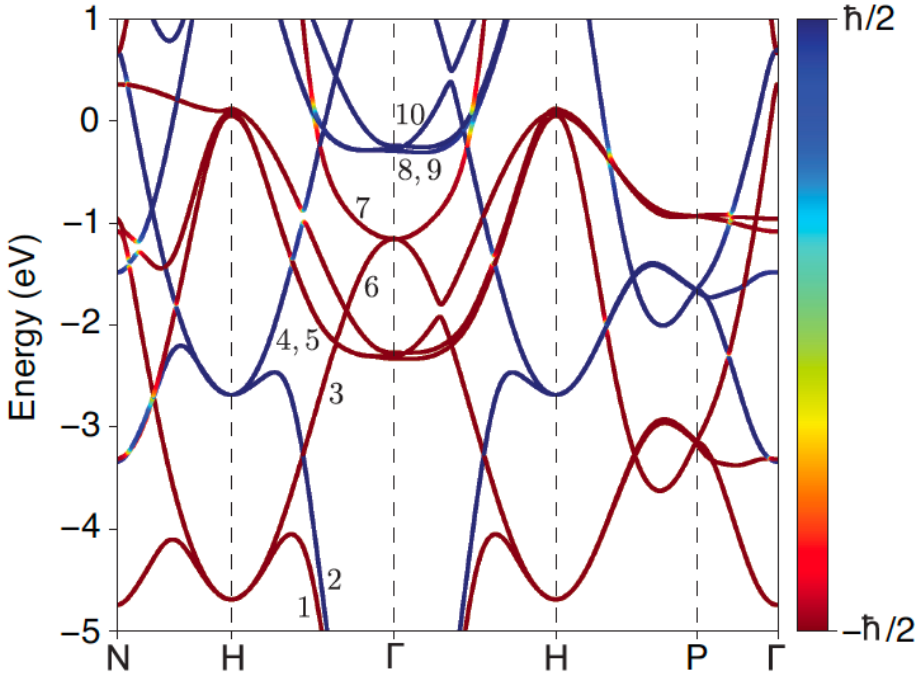

bands 6 and 7

k_x	k_y	k_z	Proj.	E	Spin	χ	Mult.
0.0	0.0	0.027	$\overline{\Gamma}$	−1.16	↓↓	−2	1
0.0	1.0	0.056	$\overline{\mathrm{M}}$	0.06	↓↓	−1	1
0.5	0.5	0.130	$\overline{\mathrm{X}}$	−0.96	↓↓	+1	2
0.180	0.820	0.180	$\overline{\mathrm{X}}\,\overline{\mathrm{M}}$	−0.34	∼↓↓	+1	4
0.074	0.322	0.242	gen.	−1.01	↑↓	−1	8
0.0	0.327	0.243	$\overline{\Gamma}\,\overline{\mathrm{M}}$	−0.99	↑↓	+1	4
0.0	0.583	0.284	$\overline{\Gamma}\,\overline{\mathrm{M}}$	−0.87	↓↓	+1	4
0.0	0.217	0.316	$\overline{\Gamma}\,\overline{\mathrm{M}}$	−0.99	↑↑	+1	4
0.135	0.662	0.338	gen.	−1.07	↓↓	−1	8
0.0	0.365	0.365	$\overline{\Gamma}\,\overline{\mathrm{M}}$	−1.02	↑↑	−1	4
0.118	0.118	0.429	$\overline{\Gamma}\,\overline{\mathrm{X}}$	−0.84	↑↓	−1	4
0.0	1.0	0.446	$\overline{\mathrm{M}}$	−0.94	↑↓	+1	1

bands 9 and 10

k_x	k_y	k_z	Proj.	E	Spin	χ	Mult.
0.0	1.0	0.047	$\overline{\mathrm{M}}$	2.35	↑↑	+1	1
0.0	0.0	0.065	$\overline{\Gamma}$	−0.25	↑↑	+1	1
0.188	0.812	0.188	$\overline{\mathrm{X}}\,\overline{\mathrm{M}}$	1.85	↑↑	−1	4
0.322	0.322	0.331	$\overline{\Gamma}\,\overline{\mathrm{X}}$	1.81	↑↓	+1	4
0.0	0.0	0.428	$\overline{\Gamma}$	−0.06	↑↑	−1	1
0.233	0.233	0.446	$\overline{\Gamma}\,\overline{\mathrm{X}}$	1.39	↑↑	−1	4
0.0	0.0	0.480	$\overline{\Gamma}$	0.07	∼↑↑	+2	1

D. Gosalbez-Martinez, I. Souza, D. Vanderbilt, PRB 92, 085138 (2015)

Breakdown of the Fermi surface of bcc iron

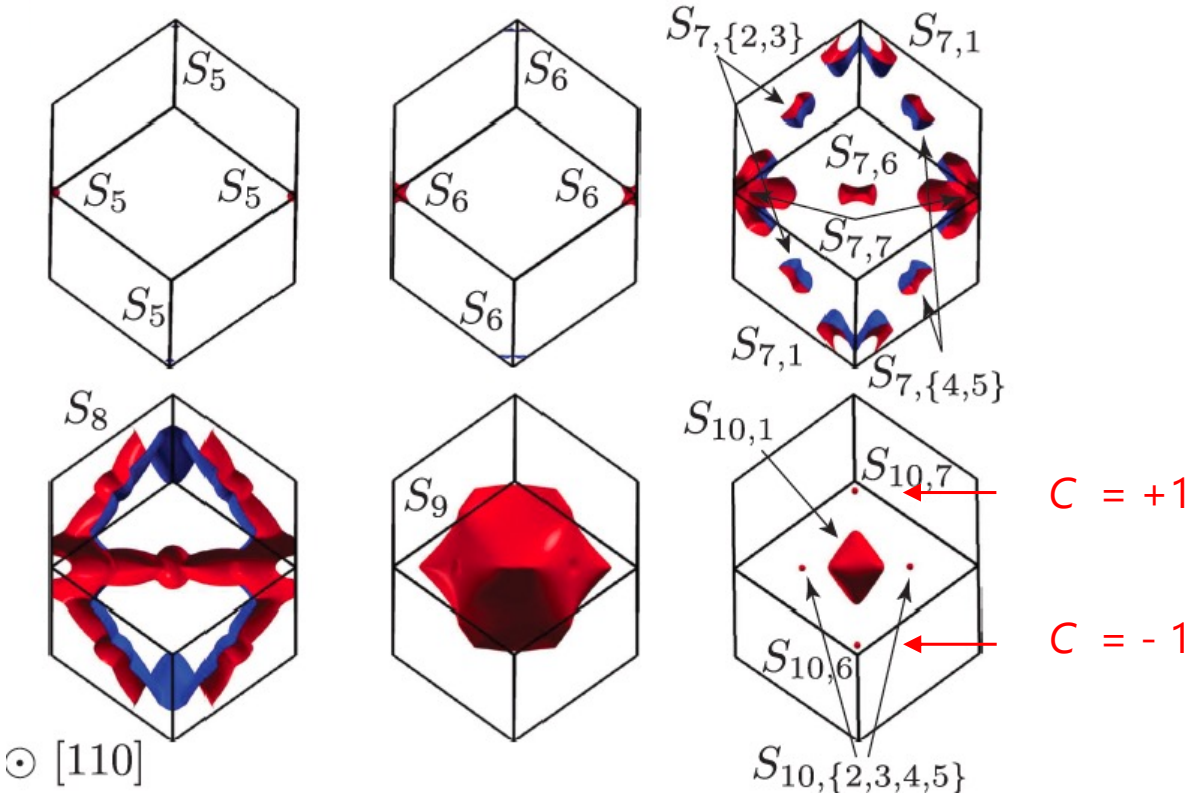

D. Gosalbez-Martinez, I. Souza, D. Vanderbilt, PRB 92, 085138 (2015)
D. Gosalbez-Martinez, G. Autés, O. V. Yazyev, PRB 102, 035419 (2020)

Breakdown of the Fermi surface of bcc iron

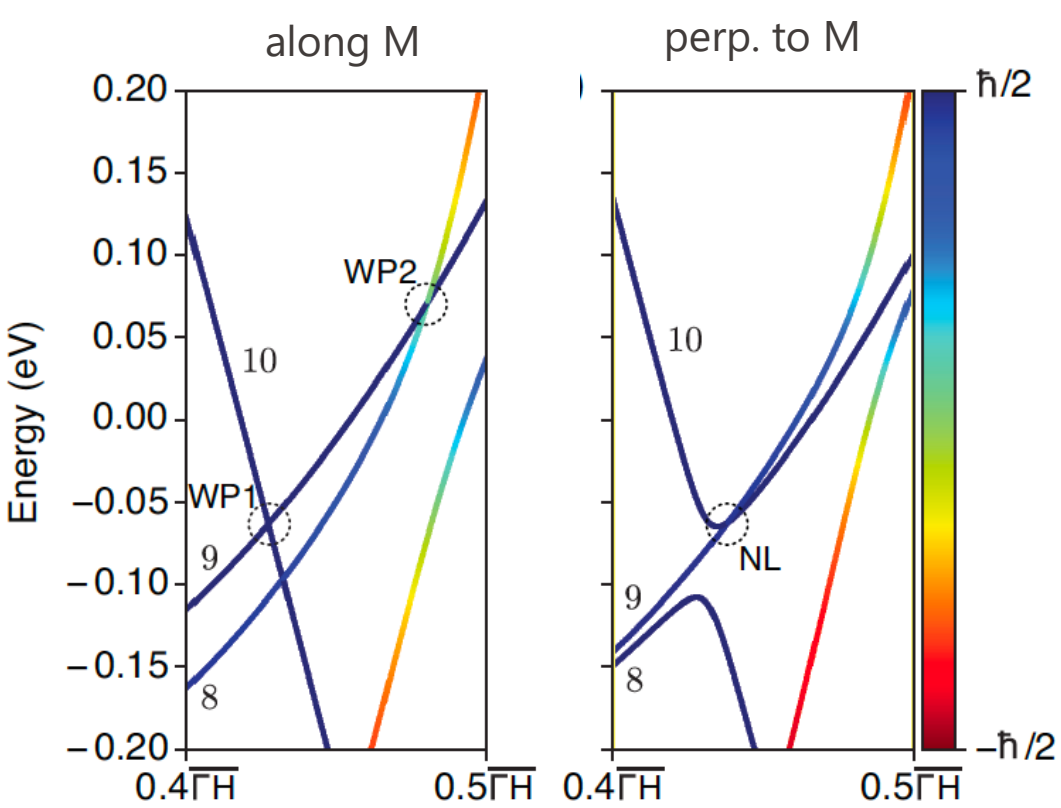

Elementary Weyl nodes WP1

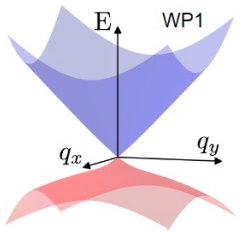

$\chi = \pm 1$

Double Weyl nodes WP2

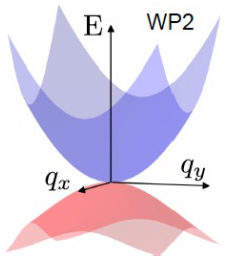

$\chi = \pm 2$

Nodal line NL

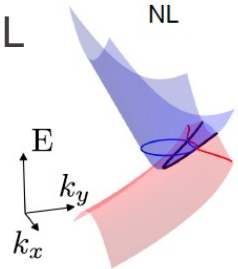

D. Gosalbez-Martinez, G. Autés, O. V. Yazyev, PRB 102, 035419 (2020)

Surface electronic structure of bcc iron

(110) surface
magnetization along [001]

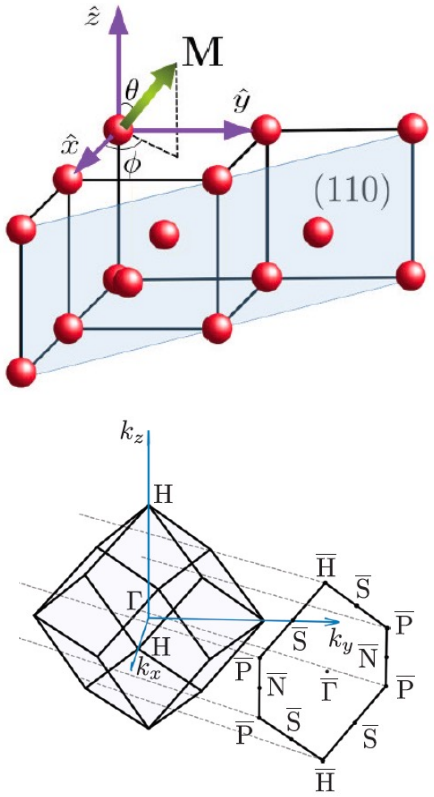

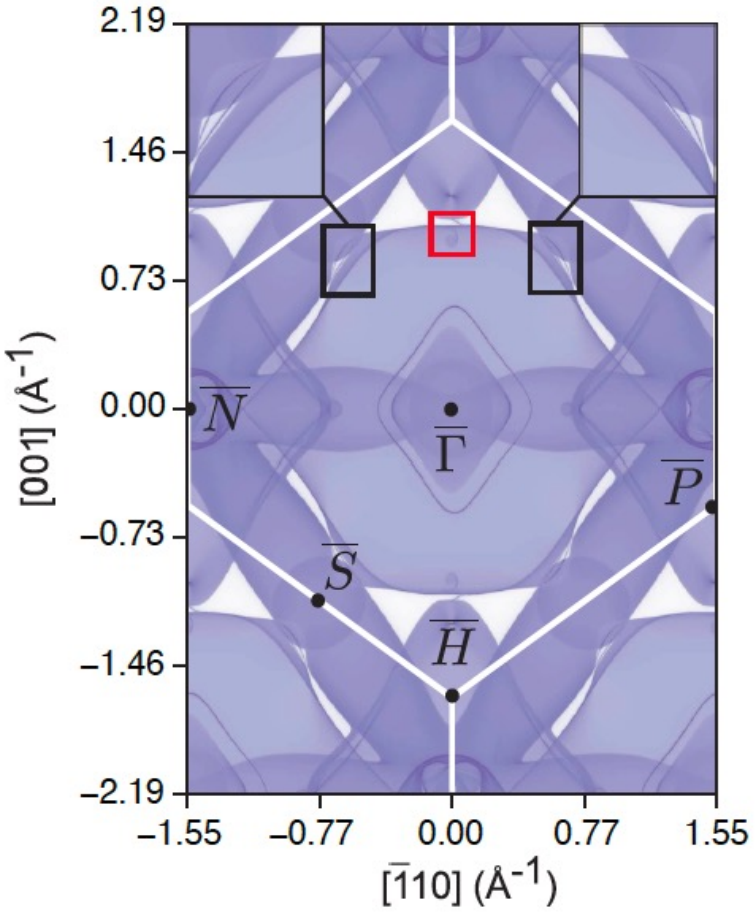

D. Gosalbez-Martinez, G. Autés, O. V. Yazyev, PRB 102, 035419 (2020)

Surface electronic structure of bcc iron

- Close-up on the topological surface resonances

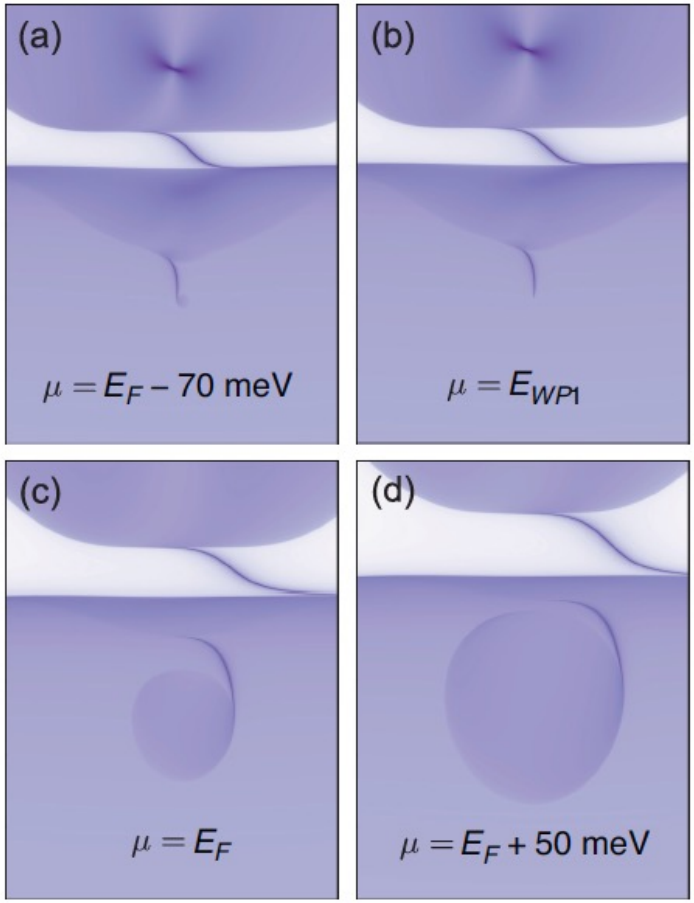

D. Gosalbez-Martinez, G. Autés, O. V. Yazyev, PRB 102, 035419 (2020)

Topological phase transition

- Topological phase transition driven by tilting magnetization direction

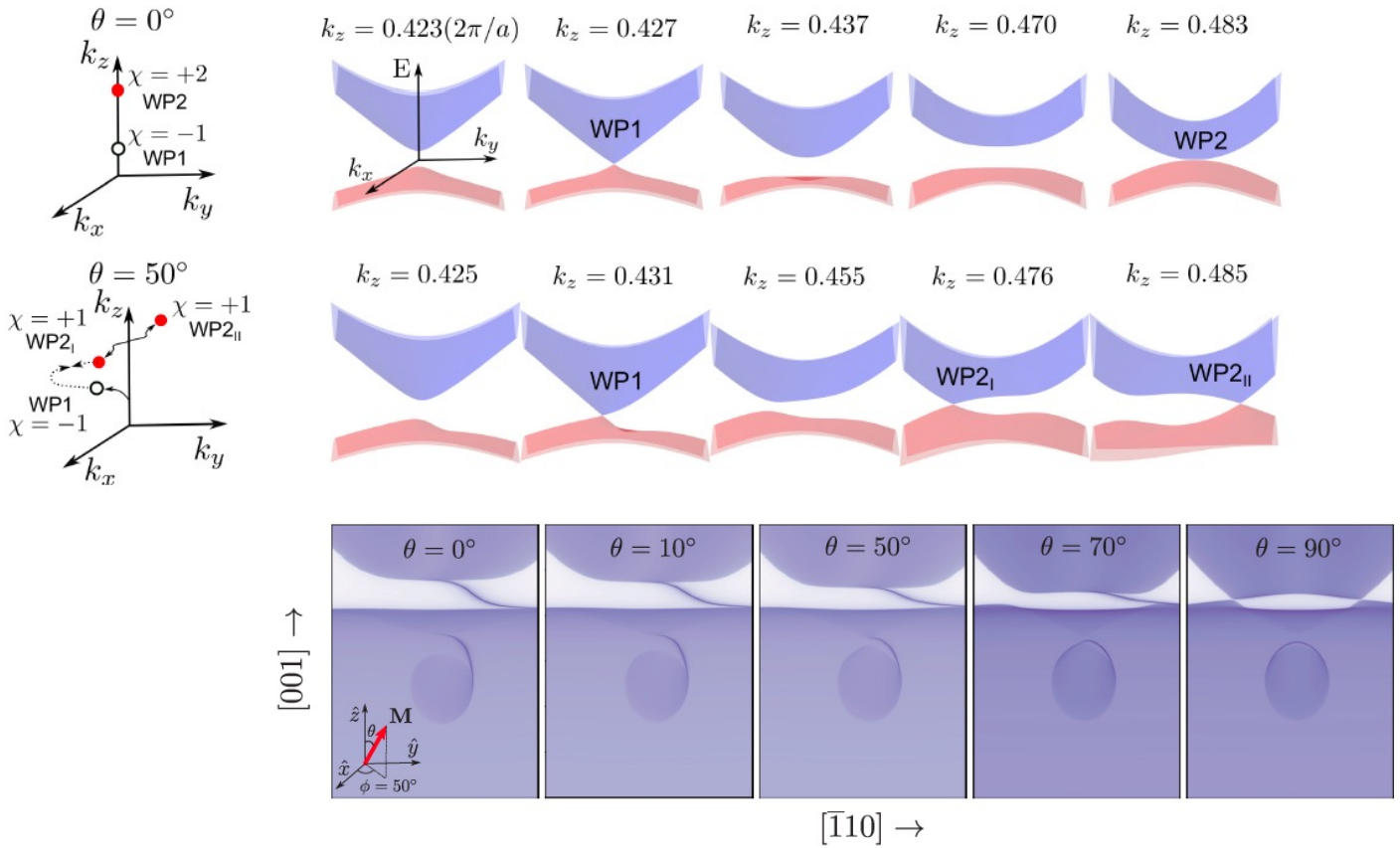

D. Gosalbez-Martinez, G. Autés, O. V. Yazyev, PRB 102, 035419 (2020)

Acknowledgments


Gabriel Autès (Lausanne)


Quansheng Wu (Lausanne)


Shengnan Zhang (Lausanne)


Hyungjun Lee (Lausanne)


Daniel Gosalbez Martinez (Lausanne)

Theory: Hyungjun Lee, Yuting Qian (Lausanne),
Dominik Gresch, Alexey Soluyanov (Zurich)
Nicola Marzari and his group (EPFL), Yi Liu (Beijing)

Experiments: Marco Grioni, Laszlo Forro, Andrea Pisoni, Alberto Crepaldi (Lausanne),
Anna Isaeva (Dresden), Luca Moreschini, Eli Rotenberg, Aaron Bostwick, Jonathan Denlinger,
Alessandra Lanzara (Berkeley), Taisia Filatova, Alexey Kuznetsov (Moscow), Nan Xu, Ming Shi (PSI)

Funding

FNSNF Swiss National Science Foundation
European Research Council erc
MARVEL MATERIALS REVOLUTION

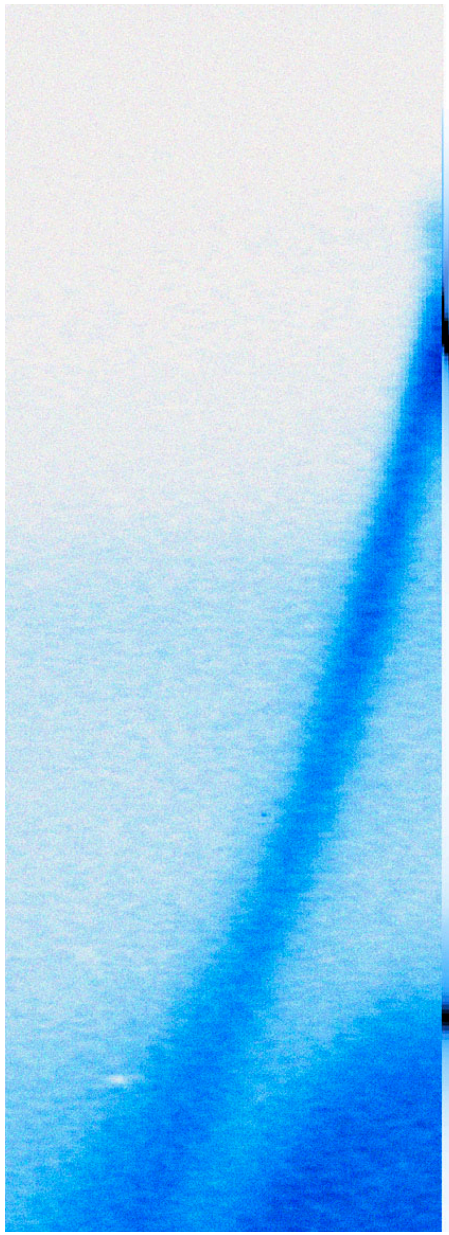

Thank you